IEEE Access
Multidisciplinary ⋮ Rapid Review ⋮ Open Access Journal

Received October 24, 2020, accepted November 16, 2020, date of publication November 27, 2020,
date of current version December 14, 2020.

Digital Object Identifier 10.1109/ACCESS.2020.3041217

A Review on Transverse Flux Permanent Magnet Machines for Wind Power Applications

RAJESH KUMAR[1], (Member, IEEE), ZI-QIANG ZHU[1], (Fellow, IEEE), ALEXANDER DUKE[2], ARWYN THOMAS[2], RICHARD CLARK[2], ZIAD AZAR[2], AND ZHAN-YUAN WU[2]

[1]Department of Electronic and Electrical Engineering, The University of Sheffield, Sheffield S1 3JD, U.K.
[2]Sheffield Siemens Gamesa Renewable Energy Research Centre, Sheffield S3 7HQ, U.K.

Corresponding author: Zi-Qiang Zhu (z.q.zhu@sheffield.ac.uk)

This research work was supported by UK Engineering and Physical Sciences Research Council (EPSRC) Prosperity Partnership "A New Partnership in Offshore Wind" under Grant No. EP/R004900/1.

ABSTRACT Transverse flux permanent magnet (TFPM) machines are a potential candidate for direct-drive wind power application due to high torque and power densities. The operating principle of TFPM machines is firstly described with various topologies available in literature, with the placement of magnets as a criterion for the classification of TFPM machine topologies. This review includes characteristics, power factor improvement, cogging torque minimization, material consideration, modelling techniques, and scalability. Different wind turbine concepts with direct-drive machines, control techniques and power converter topologies are also considered in this paper.

INDEX TERMS Permanent magnet, topologies, transverse flux, and wind power.

I. INTRODUCTION

The limited amount of fossil fuel and rising concern over global warming have made it necessary to harvest renewable energy. The wind energy became the world's fastest-growing sustainable power source due to tremendous growth during the last three decades [1]. According to the world wind energy association (WWEA), the overall capacity of all wind turbines installed worldwide by end of 2020 will reach 1260 GW, which is around 12% of the world's energy consumption. To make wind energy more attractive and competitive, technological developments should be conducted on wind turbine concepts and the generator system [2].

The rapid development in modern wind power conversion technology has been seen from the 1990s. Various wind turbine concepts and control techniques have been developed for maximizing the reliability and efficiency while reducing overall cost. There are three types of classical generator systems for large wind turbines [3]. The first type is a fixed-speed wind turbine system where the generator system employs a standard squirrel-cage induction generator (SCIG) and a multi-stage gearbox along with a direct connection to gird [4]. The second type has two variants, i.e. limited variable speed concept and variable speed concept with partial scale converter. The limited variable speed concept employs a wound rotor induction generator (WRIG) with variable rotor resistance through a power electronics converter and pitch control method [5]. The variable speed wind turbine system with a partially-rated converter has a multiple-stage gearbox and a doubly-fed induction generator (DFIG). The rating of the power electronics converter is only 25-30% of the generator capacity [6]. The last type is the gearless, i.e. direct-drive, variable speed wind turbine system. The direct-drive generator system normally comprises of a low speed and high torque synchronous generator with a full-scale power converter [7].

Gearbox failure and its frequent maintenance are two big concerns in geared wind turbine configuration. The direct-drive generator is more fascinating in terms of energy yield, simplified drive train, low maintenance, high efficiency, and reliability compared to the geared generators [8]. These direct-drive generators operate at a low speed and require large torque to produce the desired power, which usually uses a large air gap diameter of the generator and makes the direct-drive concept expensive and heavy. Furthermore, a fully rated power converter is required for the grid connection which introduces additional cost and losses [9]. Various investigations have been carried out to analyze different kinds of generators suitable for direct-drive wind turbine applications. It was discovered that the permanent magnet synchronous

The associate editor coordinating the review of this manuscript and approving it for publication was Atif Iqbal.

generator (PMSG) is the most appropriate solution for this purpose with higher energy yield, better reliability, higher torque-to-cost ratio, higher efficiency and less weight than the electrically excited synchronous generator (EESG) [10].

According to the direction of flux, the PMSG can be classified into the axial flux permanent magnet (AFPM) machine, the radial flux permanent magnet (RFPM) machine, and the TFPM machine [11]. The AFPM machine has qualities such as short axial length and higher torque/volume ratio while the main disadvantages of this machine are structural complexity and instability [12]. The RFPM machine is structurally stable with a high torque to mass ratio. Thus, most of the low-speed megawatt generators available in the market are RFPM machines [13]. The significant difference between TFPM machines and conventional machines is that the TFPM machine permits an expansion of space for the armature windings without diminishing the available space for the main magnetic flux [14]. The TFPM machine can also be made with an exceptionally small pole pitch compared with other machines. This feature permits TFPM machines to have higher torque density compared with AFPM and RFPM machines [15]. The disadvantages related to TFPM machines incorporate a complicated 3-dimensional structure, low power factor, and high cogging torque [16].

This paper deals with a thorough investigation of the TFPM machine for wind power applications. The paper is organized as follows. Initially, different wind turbine concepts are discussed in detail with special attention given to the direct-drive PM machine. Then, various topologies of the TFPM machine available in literature are reviewed thoroughly. The evaluation of the TFPM machine is carried out by considering the various factors. Finally, modelling techniques used to estimate the performance of a TFPM machine are analyzed comprehensively.

II. WIND TURBINE CONCEPT

The most commonly applied wind turbine concepts can be classified according to the rotational speed, the power regulation method, and the drive train construction [17]. In this section, the consideration is mainly given to the standard wind turbine configurations existing in the market, with their specific benefits and drawbacks.

A. FIXED SPEED

During the last decades, most wind turbine systems operate at constant speed. This traditional system was employed by many Danish wind turbine manufacturers during the early 1990s. Therefore, it is also known as the Danish concept. This fixed speed system consists of a three-stage gearbox and a SCIG directly connected to the utility grid through a transformer as illustrated in Fig. 1. This idea is extended by including a capacitive bank for the reactive power compensation. The smoother grid connection is obtained by integrating a soft-starter. Moreover, a pole changeable SCIG has been utilized for two rotation speeds. This concept has been

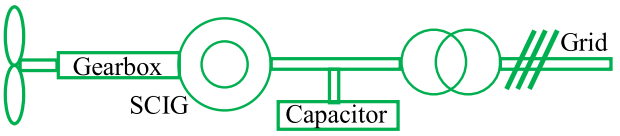

FIGURE 1. Schematic of fixed speed concept.

used by various manufacturers, such as Vestas, Made, and Nordex [18].

This system is a robust, simple, and cheap option for large scale production. Additionally, it enables the stall regulated machine to operate at a fixed speed when it is connected to a large gird, which provides a stable control frequency. However, the speed is uncontrollable with a narrow range of variation. The generator operation is possible for speed higher than synchronous speed. This leads to higher dissipation of electrical energy due to higher slip. The direct conversion of wind speed fluctuations into electromechanical torque variation is responsible for mechanical and fatigue stresses on the system in the fixed speed concept. Besides, the three-stage gearbox in the nacelle is heavier and requires a large fraction of the investment cost and maintenance [19].

B. LIMITED VARIABLE SPEED

This concept is also named as the Optislip concept, mainly applied by Vestas. It uses a wound rotor induction generator (WRIG) which is directly connected to the grid. The rotor winding of the generator is connected in series with a controlled resistance, whose size defines the range of the variable speed (typically 0-10% above synchronous speed). A capacitor bank performs the reactive power compensation and a smooth grid connection occurs by means of a soft-starter as depicted in Fig. 2.

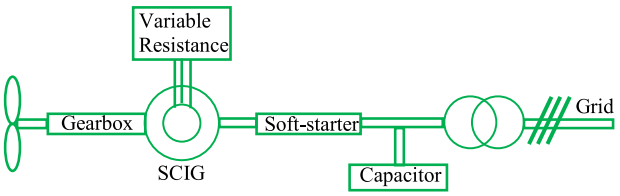

FIGURE 2. Scheme of limited variable speed concept (Optislip).

The variable-speed operation is obtained by controlling the energy from the WRIG rotor [20]. The higher power extraction by the rotor with lower efficiency due to increment in variable speed range and slip requires a higher rated external resistor for power dissipation. Therefore, the dynamic speed control range is dependent on energy extracted from the external resistor (dumped as heat loss) and the size of the variable rotor resistance [21].

C. VARIABLE SPEED (PARTIAL SCALE CONVERTER)

This setup commonly called a DFIG concept. This setup consists of a multistage gearbox, a cost-effective WRIG, and a partial scale converter feeding the rotor winding as illustrated

in Fig. 3. The stator is directly connected to the grid while the rotor is connected through a power electronics converter. The rotor speed and frequency are controlled via a power converter. The wide speed range operation depending on the size of the converter is possible through this concept. The rating of the power converter is only 25%-30% of the rated power, enabling a speed range from roughly 60% to 110% of the rated speed [22]. This is sufficient for a good energy yield because the tip speed ratio can be kept optimal for a large part of the operating range. This concept is used by many manufacturers such as Vestas, Siemens, Gamesa, Repower in the market.

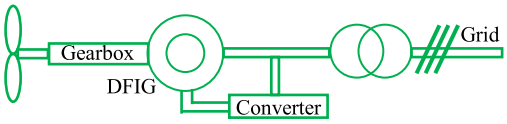

FIGURE 3. Layout of variable speed concept with DFIG.

The rotor energy can be directly injected into the grid by the converter compared to the Optislip concept. Besides, the smooth grid connection and reactive power compensation can be performed by the power electronics converter. However, DFIG has some drawbacks such as a limited supply of reactive power for the compensation of the grid power factor. The gearbox is responsible for heat dissipation due to friction, regular maintenance, and audible noise. The requirement of a slip ring and brushes may cause machine failure and electrical losses. Furthermore, power electronics converter and drive train of wind turbine need to be protected from large stator current and high torque under grid fault condition [23]–[24].

D. VARIABLE SPEED DIRECT-DRIVE

It is a well-known fact that gearbox failure and its frequent maintenance are two major concerns in a geared wind turbine concept. The solution to these problems lies in a variable speed wind turbine with a direct-drive generator connected to the grid through a full-scale converter. The inverse relationship of torque T, and mechanical angular speed Ω, the power P of the generator is scaled up by increasing the torque [25]:

$$P = T\Omega \tag{1}$$

The torque of the generator is proportional to the tangential force F and the air gap diameter D_g. The tangential force can be defined as the multiplication of the air gap area and the tangential force density F_d. Thus, the generator can also be represented as [26]:

$$P = \frac{\pi}{2} F_d D_g^2 l \Omega \tag{2}$$

where l represents the axial length of the generator. Since the torque is proportional to the square of the air gap diameter, the direct-drive generator has a larger diameter to produce higher torque. The large air gap diameter offers a multi-pole structure with reasonable pole pitch at low speed and high torque operation. Moreover, the direct-drive wind turbine has a simplified drive train, high efficiency, high reliability, and availability by going gearless [27]. However, there are few flaws in this concept such as large diameter, large mass, and high cost [28]. The direct-drive generators used in the market are classified as follows:

1) ELECTRICALLY EXCITED SYNCHRONOUS GENERATOR

In this configuration, field windings located on the rotor are fed with direct current (DC) excitation while the stator carries three-phase windings. The rotor may consist of cylindrical or salient poles. The grid connection scheme of direct-drive EESG is depicted in Fig. 4. The wide range of speed is covered by taking full control of voltage amplitude and frequency through power electronics at the generator side [29]. Additionally, the opportunity of controlled flux for minimized loss at different power range can be achieved by power converter in the rotor side which regulates the excitation current. The absence of PMs made this concept cost-effective and robust under harsh atmospheric conditions. The typical manufacturer is Enercon, the largest capacity of the direct-drive EESG has been up to 4.5 MW [30].

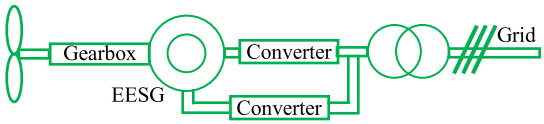

FIGURE 4. Schematic of direct-drive EESG.

The major disadvantage of EESG is the space requirement for excitation winding and pole shoes. The pole pitch must be sufficiently large for the substantial diameter-specific design, so a larger number of parts and windings make this heavyweight and costly. Furthermore, it is important to energize the rotor winding with DC, utilizing slip rings and brushes, or brushless exciter. The employment of a rotating rectifier and field losses are unavoidable [31].

2) PERMANENT MAGNET SYNCHRONOUS GENERATOR

The grid connection scheme of the PMSG for direct-drive wind turbines is shown in Fig. 5. The PMSG is excited by the PMs with a direct connection to the grid through a full-scale power electronics converter.

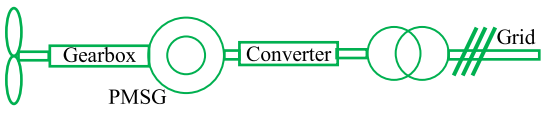

FIGURE 5. Scheme of direct-drive with PMSG.

The benefits of PM excited machine over electrically excited machine can be summarized as [32]:

- High efficiency and energy yield;
- No need for DC excitation;
- Improved thermal characteristics due to absence of field losses;

- The absence of mechanical components such as slip rings provide high reliability;
- High power to weight ratio.

However, PM machines have following drawbacks [33]:

- High cost of PM material;
- PM demagnetization at high temperature.

III. CLASSIFICATION OF DIRECT-DRIVE PM MACHINES

The PM machines are not standard off-the-shelf machines and they allow a great deal of flexibility in their geometry so that different topologies can be used. The PM machine can be classified by both the direction of the flux path and the structure. However, they are generally characterized by their direction of flux penetration, such as radial flux, axial flux, and transverse flux. Some basic features and structures from literature are briefly summarized as follows [34].

A. RADIAL FLUX PM MACHINE

This is the most common configuration in PM machines where flux lines are in the radial plane while the current flows in the axial direction as shown in Fig. 6. The type of machine is widely employed in various applications such as ship propulsion systems, wind power generation, traction, and many others [35].

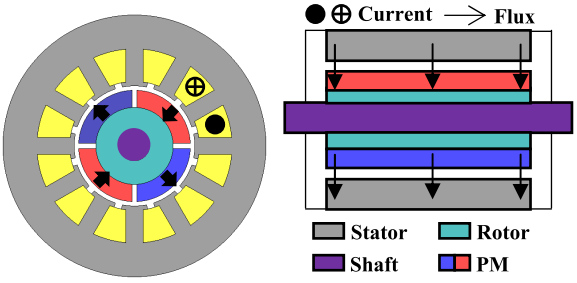

FIGURE 6. Radial flux PM machine.

For direct-drive wind turbines, the RFPM machine can operate over a wide range of operations with better performance. The air gap diameter and axial length of the machine can be chosen independently. The longer axial length and smaller diameter would cause a larger proportion of copper loss to be attributed to the end windings [36]. There are two common types of RFPM machine i.e. surface-mounted and flux concentrated RFPM machine mostly discussed in the literature [37]. The surface-mounted RFPM machine seems to be a good option for the large scale direct-drive wind turbines [38]. The remanent flux density is higher than the air gap flux density in magnets on the rotor surface compared to flux concentrated topology [39]. The comprehensive comparison of flux concentrated and surface-mounted RFPM machine has been carried out in [40]. Besides, an external rotor configuration for a large direct-drive generator is more convenient compared to the internal rotor because of ease in installation and maintenance. Additionally, higher torque density can be obtained by a large outer periphery and multi-pole structure [33].

B. AXIAL FLUX PM MACHINE

The AFPM machine is another possible solution for direct-drive applications. This machine generates magnetic flux in the axial direction instead of radial direction as shown in Fig. 7. The flux from the PM flows axially while the current flows in the radial direction. This machine features a large diameter and a relatively short axial length compared to a radial-flux PM machine [41].

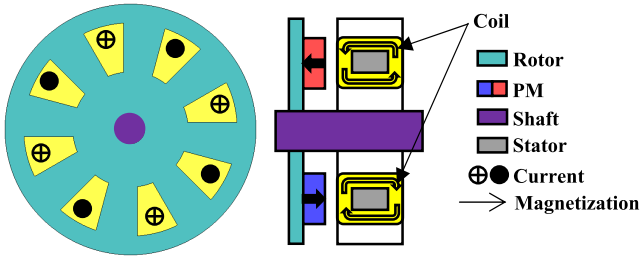

FIGURE 7. Axial flux PM machine.

The AFPM machine has some advantages compared to the RFPM machine, which are illustrated as follows [42]:

- Simple winding and short axial length;
- Low cogging torque and noise;
- High torque/volume ratio.

However, AFPM machine accompanied with some disadvantages such as [43]:

- High PM utilization with large diameter;
- Structural instability;
- Difficulty in maintaining air gap in large diameter.

The conventional slot-less AFPM machine with a single stator and dual rotor is also called a Torus machine. The electromagnetic analyses with various advantages, such as short axial length, lightweight, compact, high power to weight ratio, and suitable integration with the engine, are discussed by various authors in [44]. The direct-drive Torus for wind power has been examined based on perceived benefit for 5 kW at 200 rpm [45]. The analytical study of the initial slotted AFPM machine design with one rotor and two stators has been carried out for the power range of 10-500 kW [46]. Furthermore, a 2.7 MW AFPM machine with two PM rotors and one stator was considered for large wind turbines [47]. The comparative study was performed for various 5 MW topologies and 9-phase AFPM machine with concentrated winding [48]. The 10 MW iron-less AFPM machine was examined for offshore wind turbines with especial consideration on weight minimization [49].

C. TRANSVERSE FLUX PM MACHINE

Initially, the concept of the TFPM machine was patented by W. M. Morday in 1895. But, the development work is not carried out further because of no relative advantage. In the 1970s, some articles on the linear TFPM machine for railway application by E. R. Laithwaite *et al.* gave new life to this idea. Finally, a publication by H. Weh drew broad attention to this machine [50]. The force-producing magnetic circuit

is positioned in a plane orthogonal to the direction of motion. The simplest topology of the TFPM machine is a single-sided surface-mounted TFPM machine shown in Fig. 8.

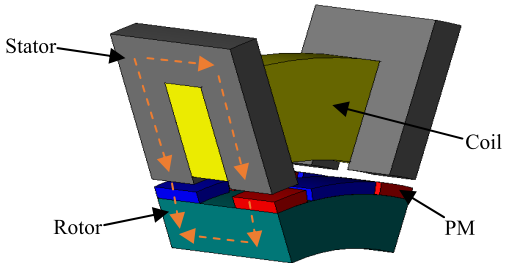

FIGURE 8. Transverse flux PM machine (one pole pair).

This machine performs like a synchronous machine. The TFPM machine has a higher torque density, separate electrical and magnetic loadings, modular structure, fault tolerance, and simple windings [51], [52]. However, this machine suffers from poor power factor, high cogging torque, high losses, and complex manufacturing [53], [54].

In order to become a prominent candidate in wind power applications, the TFPM machine should be fairly designed and compared with a conventional RFPM machine. The design procedure of the TFPM machine is presented in Fig. 9. The method is comprised of three parts, i.e. conditions, investigation, and optimization.

IV. TRANSVERSE FLUX PM MACHINE TOPOLOGIES

Several TFPM machine topologies are introduced and investigated in literature since they attracted attention in the early 1970s and later reappeared in the mid-1980s. Based on electromagnetic configuration, the TFPM machines can be categorized as follows:

- Surface-mounted and flux concentrated;
- Single-sided and double-sided;
- Single winding and dual winding;
- Inner rotor and outer rotor;
- Stator type: C/U-core, Z-core, E-core, claw pole.

In this paper, the TFPM machines are classified into surface-mounted TFPM machine and flux concentrated TFPM machine as presented in Fig. 10.

A. SURFACE-MOUNTED

The surface magnet form of the TFPM machine behaves like a non-salient synchronous machine where PM and air gap have similar permeability. The total torque has two components, the opposing cogging torque and the interaction torque component. Moreover, the surface magnet TFPM machine has a larger active air gap because of the extra air gap created by magnets [55].

1) SINGLE-SIDED

The fundamental topology shown in Fig. 11 comprises a mover core with magnets mounted on the surface. The winding is placed in C/U shaped iron core of laminated steel. The

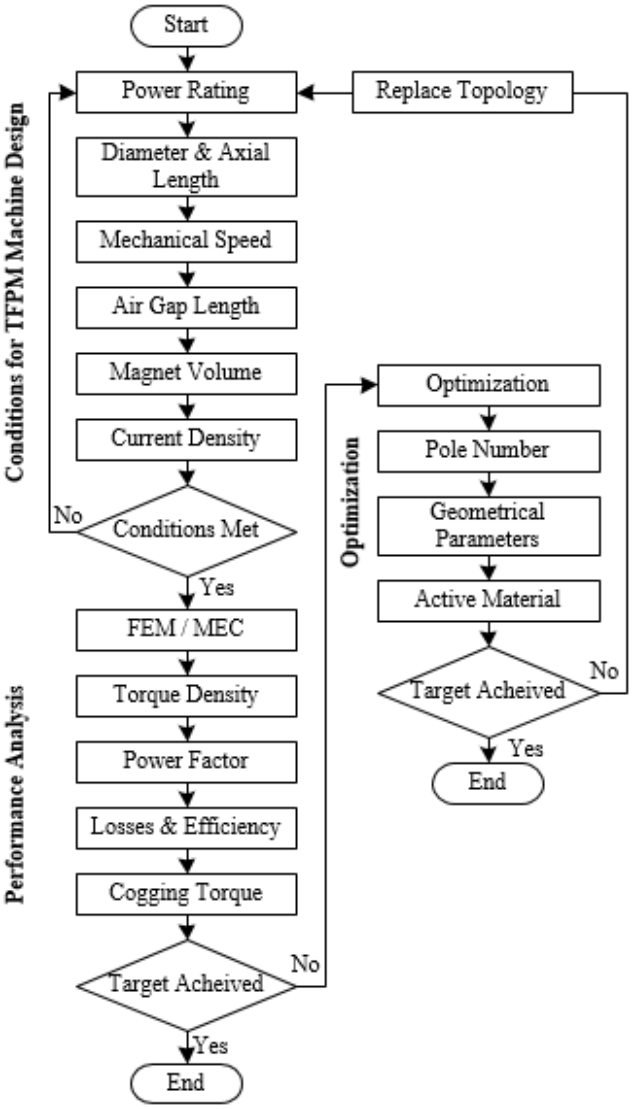

FIGURE 9. Flow chart of TFPM machine for wind power applications.

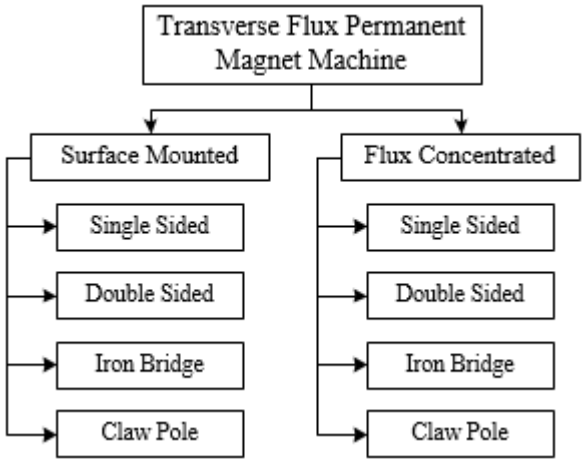

FIGURE 10. Classification of TFPM machine.

magnets magnetized with alternating polarity are displaced on the rotor, thereby generating an alternating flux in the

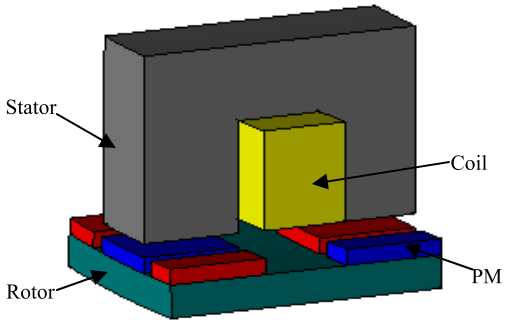

FIGURE 11. Single-sided surface-mounted TFPM machine.

TABLE 1. Performance of Single-Sided TFPM Machine for Wind Power.

Parameters	[119]	[62]	[59]	Unit
Poles	524	560	120	-
Diameter	6	2.8	0.55	m
Air Gap	6	4	1	mm
Torque	2340	-	3.8	kNm
Power	3.3	5	0.02	MW
Efficiency	92	97	93	%
Power Factor	-	-	0.51	-

stator. The flux produced by each pole pair is linked with the same global winding. In this topology, only half of the magnets are being used at one moment, while other produce flux that can lessen the flux linked with the winding. Additionally, it has high leakage reactance [56].

A two-phase TFPM machine with a static equation for the calculation of torque per volume and mass is presented in [57]. The machine has 5 times higher torque density compared to a typical induction machine. The flux linked with stator winding is 20% of the total stator flux linkage. This machine is optimized in [58] where the author showed that high flux leakage between the rotor and the stator is responsible for high q-axis reactance. The machine also suffers from opposing fringing fluxes with reduced back-EMF. An external rotor TFPM machine was developed in [59]. The outer rotor concept has high torque density with poor thermal paths for heat dissipation. Moreover, better performance with full magnet utilization is achieved by surface-mounted TFPM machine with intermediate poles (Z-machine). The output of this topology is twice higher than that of the conventional TFPM machine at the same volume. However, this machine has high 3-D leakage and high loss with poor efficiency [60]. For large wind turbines, a 5MW direct-drive TFPM machine is proposed in [61]. The magnetic equivalent circuit (MEC) of this machine is developed without considering leakage and saturation [62]. The power factor and efficiency are assumed to be 0.99 and 97% respectively. Additionally, the performance of various single-sided TFPM machines designed for wind power applications is presented in Table. 1.

2) IRON BRIDGE

To lessen the stray flux produced by inactive magnets, guiding iron bridges could be placed between the stator cores as depicted in Fig. 12. This will provide a closed magnetic path for the flux generated by each magnet that is not involved in the development of the main magnetic flux. The output power would likely be higher in this arrangement. However, the iron bridge will make the machine heavier with a decrease in available space for the stator winding and high core losses. The bridges will also cause significant leakage flux from the adjacent stator cores [63].

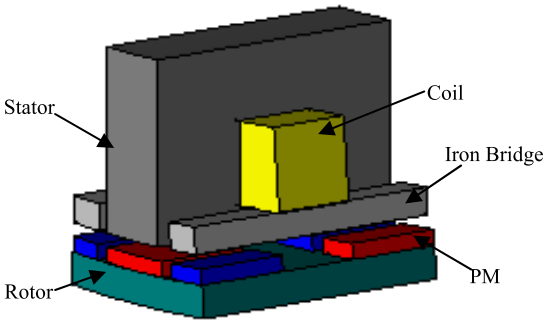

FIGURE 12. Single-sided TFPM machine with iron-bridge.

A unique design of the TFPM machine with an iron-bridge is examined in [64]. The rotor is similar to a hybrid stepping motor with an axially magnetized PM ring. The machine suffers from high cogging torque due to the high use of PM. An outer rotor generator based on the TFPM machine principle with iron-bridge was patented in [65]. The 6 kW generator has a 92% efficiency and 0.58 power factor. The main drawback of this design lies in the high flux leakage in the stator core. The same topology is optimized by inserting a semi-open slot instead of an open slot [66]. The machine has a high power factor of 0.8 with high power losses due to the eddy current induced in the iron bridge. For the reduction of magnet volume, a fall back generator is proposed in [67]. The basic structure is similar to a conventional TFPM machine with an iron bridge. However, only half of the magnets are used in this topology. The inactive magnets are removed and the magnetic flux is diverted from the return path (fall back path) through a rotor to serve the purpose of inactive magnets. Furthermore, the iron-bridge configuration is modelled and compared with the traditional TFPM machine without a bridge for large wind turbines. The iron bridges are superior in terms of magnet utilization by 84% [68]. The author in [69] discovered that the flux in the rotor back iron is guided in the longitudinal plane due to the magnets and iron-bridge offering a lower reluctance path. In addition, this topology is widely investigated for wind power applications due to the better utilization of magnets. The performance of single-sided TFPM machines with iron-bridge for different power rating is illustrated in Table. 2.

3) DOUBLE-SIDED

An alternative scheme to employ all magnets in the machine is to utilize two stators, one on each side of the rotor, as presented in Fig. 13. This topology consists of two sets of

TABLE 2. Performance of Single-Sided TFPM Machine with Iron-Bridge.

Parameters	[70]	[66]	[65]	[119]	[68]	Unit
Poles	70	16	36	524	720	-
Diameter	0.56	0.15	0.21	6	10.5	m
Air Gap	1	1	1	6	7	mm
Torque	0.03	0.019	-	9432	-	kNm
Power	0.001	0.0018	0.006	4.9	10	MW
Efficiency	88	90	90	92	97	%
Power Factor	0.92	0.8	0.58	-	-	-

C/U shaped cores per pole pair, with the winding placed in the slots. The magnets are embedded in the rotor cores. The performance of the machine compared to a single-sided design is improved by two-fold. To provide a return path for the magnetic flux, iron bridges can be added to this topology. The double-sided surface-mounted TFPM machine has a higher VA rating for the same volume and relative pole pitch compared to a single-sided TFPM machine. However, the drawback is the increased complexity associated with constructing the active rotor parts as they have to be supported in a cantilevered arrangement [70].

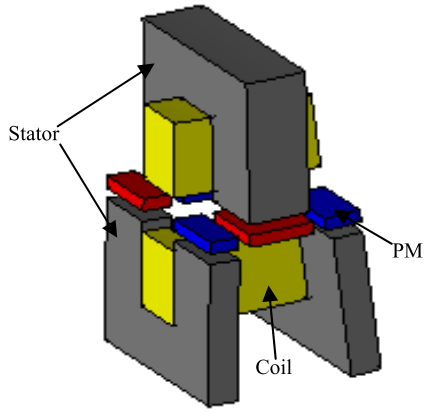

FIGURE 13. Double-sided TFPM machine with iron-bridge.

This topology can also be designed with only one winding with nearly the same torque production as in the double-sided TFPM machine with two windings. It has the benefit of a simple mechanical structure and shorter outer diameter [71]. The double-sided TFPM machine was initially proposed in [72]. The comparison is also carried out for force density between various PM machines. Additionally, a double-sided modular TFPM machine with axial flux configuration has been proposed for wind turbine generators [73]. However, this topology has a complicated structure with leakage at the rotor pole.

4) CLAW POLE

Another approach is to twist the stator core in such a way that all magnets are employed simultaneously as depicted in Fig. 14. This type of arrangement is called a claw pole. It can be noted from the figure that only half of the stator tooth faces the pole area at the same time. This is done for decreasing the armature flux leakage between the twisted stator teeth. The shorter tooth span will cause saturation in the stator tip with low magnetic flux linkage. Additionally, this machine is mechanically unstable due to the complex structure [74].

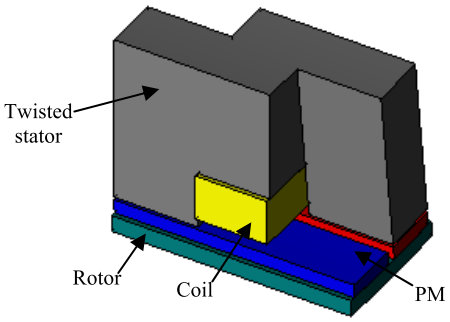

FIGURE 14. Single-sided surface-mounted claw pole TFPM machine.

In [75], different claw pole geometries have been investigated for high torque density and better power factor. The axially shortened claws limit the armature inter-polar flux leakage. A single-sided claw pole TFPM machine was proposed for better magnet utilization [76]. The claw structure was made with soft magnetic composite (SMC) material. The machine is optimized through the analytical and finite element method (FEM). Recently, a single-sided TFPM machine with an outer rotor and non-overlapping stator pole is proposed in [77]. This novel topology has 100% magnet and winding utilization without reducing the conductor space.

B. FLUX CONCENTRATED

In flux concentrated setup, the inset magnets allow a significant increase in the air gap flux density because magnetic flux is concentrated to a flux path with a smaller cross-section than the magnet. The relationship between magnet and pole face area is given by flux focusing factor as [78].

$$k_f = \frac{B_g}{B_m} = \frac{A_m}{A_p} \tag{3}$$

where k_f is the flux focusing factor, B_g is the air gap flux density, B_m is the magnet working flux density, A_m is the magnet area and A_p is the pole face area. The air gap flux density can increase above the remanent flux density of PM used in the magnetic circuit. This type of design has 20% to 50% higher torque and improved power factor compared to surface magnet design. Furthermore, the placement of magnets inside the magnetic circuit produces saliency for an additional component of torque, i.e. reluctance torque which facilitates a wider speed range at constant power operation. Thus, the total torque is sum of PM and reluctance torque components. Besides, it has complicated construction and lower robustness [79].

1) SINGLE-SIDED

The single-sided flux concentrated TFPM machine depicted in Fig. 15 uses only half of the magnets at each time. The benefit of this topology is an improvement in performance with a reduction in active material over surface-mounted configuration. On the other hand, it has a more complicated rotor assembly. The toothed rotor construction can be utilized for mechanical stability [80].

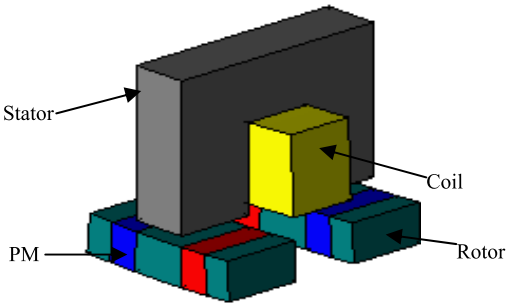

FIGURE 15. Single-sided flux concentrated TFPM machine.

For the wind power generator, a comparison of two optimized 5 MW TFPM machines is carried out for active mass reduction [81]. The C-core geometry utilizes less PM volume along with an 11% reduction in active mass compared to U-core. A 5 MW RFPM machine and four different TFPM machines have been examined on the basis of cost, mass, and copper loss. The C-core TFPM machine with a double-sided air gap and single winding seems to be the best concept considering all criteria. Besides, the analytical modelling of the RFPM machine and the TFPM machine discussed by neglecting saturation and considering the power factor to be 1 [82]. The short flux path with the plural module concept for the TFPM machine is discussed in [83]. This concept is 60% lighter than the RFPM machine for the same power level with a drawback of higher current density. The design process of SMC based outer rotor TFPM machine for light electrical vehicles is illustrated in [84]. The optimization process of the TFPM machine with a dual rotor is discussed in [85]. The d and q-axis magnetic flux and torque for the same topology are deduced through the MEC. Two different TFPM machine topologies with distributed windings have been modelled via FEM in [86]. The prototype development of TFPM machine with SMC and formed lamination for aerospace applications are presented in [87]. Additionally, this configuration has also been analyzed broadly for wind power due to high torque density and better power factor compared to the surface mounted TFPM machine. For different power levels, the performance of single-sided TFPM machines is presented in Table. 3.

2) IRON BRIDGE

To ensure complete utilization of magnets in conventional single-sided flux concentrated TFPM machine, the stator bridges are placed over the inactive magnets to close the magnetic circuit as depicted in Fig. 16.

TABLE 3. Performance of Single-Sided Flux Concentrated TFPM Machine.

Parameters	[81]	[83]	[159]	Unit
Poles	300	194	150	-
Diameter	5.2	6.14	10.4	m
Air Gap	5.2	6.14	7.8	mm
Torque	3183	-	8595	kNm
Power	5	5.5	10	MW
Efficiency	-	-	-	%
Power Factor	-	-	-	-

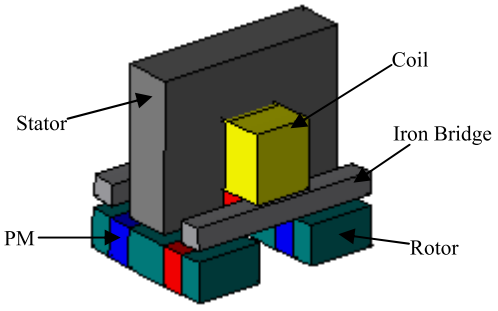

FIGURE 16. Flux concentrated TFPM machine with iron-bridge.

For the wind power generator, the study of the TFPM machine with a toothed rotor is carried out in [88]. The leakage between stator and iron-bridge is lessened by modifying the iron-bridge into a trapezium and C-core stator into a horseshoe with a foot. Moreover, the diameter below 1 m is beneficial for the TFPM machine compared to the PM synchronous machine for torque and mass benefit. In [89], a new design of the TFPM machine with E and I shape stator core is presented for wind power. The disk shape rotor is selected because of low inductance and better power factor compared to the cylindrical rotor. The coil is wrapped around the middle arm of the E shape core while PM embraced in the rotor. The comparison of different single-sided flux concentrated TFPM machines with and without iron-bridge is performed in [86].

3) DOUBLE-SIDED

The first double-sided TFPM machine with dual winding and U-core stator shown in Fig. 17 was proposed in [90]. The better usage of magnets at any specific time produces better performance. However, this structure is mechanically unstable due to complex construction and moving magnets. The same topology is converted from double winding to single winding without affecting the torque rating of the machine. The difficulty of mounting top winding has been eradicated with a reduction in the outer diameter. Furthermore, the double-sided TFPM machine with a single winding and C-core arrangement is obtained from the U-core concept [91]. The no-load flux linkage of this topology is comparable to the U-core version under the same dimension with the elimination of 50% magnets and air gaps. However, the saturating

MMF of the stator coil is reduced by a factor of 2; the torque density of the machine is roughly decreased by half. The analytical modelling of C-core configuration is developed without considering the saturation effect [92].

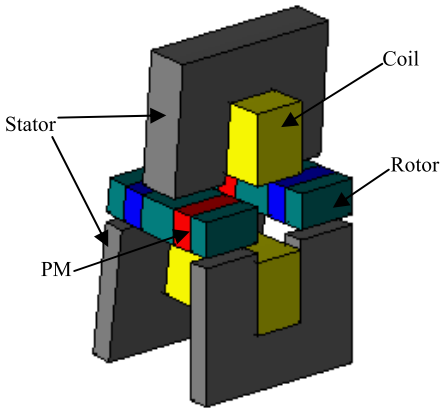

FIGURE 17. Double-sided flux concentrated TFPM machine.

The E-core TFPM machine consists of two separate stator parts with a reduction in axial length of the rotor. The C-core stator part surrounds the winding while U-core is placed in between two windings. This concept has the same expected performance and drawback as the conventional double-sided TFPM machine [93]. For wind power, a modular double-sided TFPM machine with a quasi U-shaped stator with ring winding is presented in [94]. The rotor consists of ferrite magnets. The impact of key geometric parameters on the torque production is also mentioned in this paper. The E-core TFPM machine with pole winding and ferrite magnet is developed in [95]. Additionally, the Halbach array magnet arrangement is introduced for lessening the inter-polar leakage in a double-sided TFPM machine [96]. This arrangement increases the flux linkage by 90%. The double-sided TFPM machine with iron-bridge for wind power applications is proposed in [97]. The machine comprises of C-core stator, pancake shape rotor and I shape magnetic shunt. The machine is optimized for better power factor and reduced volume. However, it has high PM volume and saturation in the iron core. Recently, various double-sided TFPM machine have been investigated for wind power applications by taking the advantages of better utilization of magnets, higher torque density and improved power factor. The performance of double-sided TFPM machines is given in Table. 4.

TABLE 4. Performance of Double-Sided Flux Concentrated TFPM Machine.

Parameters	[94]	[95]	[97]	[96]	Unit
Poles	30	30	150	24	-
Diameter	0.225	0.225	8.77	0.166	m
Air Gap	1	1	8	1	mm
Torque	0.029	0.029	9906	-	kNm
Power	0.0012	0.0012	10	0.0012	MW
Efficiency	91	88.2	96	90	%
Power Factor	0.2	0.67	0.66	0.89	-

4) CLAW POLE

The claw pole TFPM machine topology shown in Fig. 18 tries to combine the simplicity of single-sided topology with increased power density of double-sided TFPM machine [98]. However, the stator provides a short circuit part for the magnetic flux with saturation. The complicated design requires SMC material for manufacturing [99].

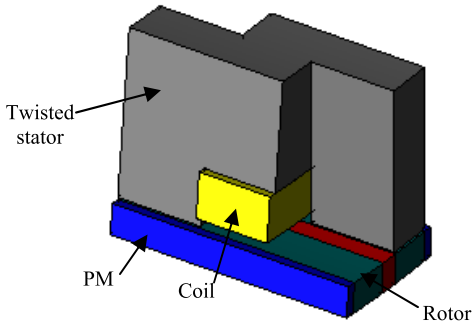

FIGURE 18. Flux concentrated claw pole TFPM machine.

A 5 MW TFPM machine was designed for wind power applications [100]. The comparison was made for various TFPM machine topologies. The V-type embedded magnets with claw pole stator achieved the highest torque density. In [101], a single-phase TFPM machine is fabricated for the driving system of a green mechanical press. The claws and back iron of the stator have different direction of lamination. The energy loss of this machine is 30% less than the mechanical press. The impact of stator pole overlapping is discussed in [75]. The 6% increment in torque is obtained at a 30% overlap of the stator pole. Furthermore, the optimization process of the claw pole TFPM machine for bicycle application is illustrated in [102].

C. MISCELLANEOUS TOPOLOGIES

There are some TFPM machines which differ from the previously mentioned topologies are discussed in this section.

1) FLUX SWITCHING

In this configuration, all MMF sources are located on the stator while the rotor has a salient structure as shown in Fig. 19. The PM flux switches clockwise or counterclockwise around the coil. This configuration combines the high torque density of the TFPM machine and mechanically robust structure of the transverse reluctance machine. The magnet utilization of the flux switch TFPM machine is better than other TFPM machines. The laminated steel material is employed for cores when 50% magnets utilize at any time. The SMC is needed for a topology that utilizes all magnets [70].

For low-speed wind generators, a 1.3 kW TFPM machine based on the flux switching principle is presented in [103]. The computation of this machine has been performed only

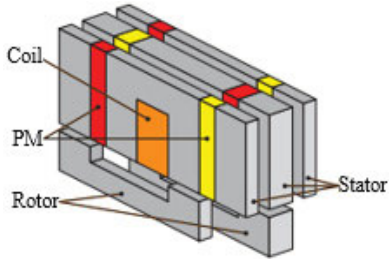

FIGURE 19. Flux switching TFPM machine [70].

at no-load condition. The cogging of this machine is significantly influenced by stator and rotor core circumferential width to pole pitch. In addition, a 380 W three-phase prototype is manufactured for validation purposes. A comparison of two flux switching TFPM machines with SMC cores and ferrite magnets is performed in [104]. The difference between d- and q-axis inductances is small and only the PM component contributes to the main torque. The initial design of flux switching TFPM machine with SMC cores and ferrite magnets is proposed in [105]. Preliminary analysis shows that it has higher cogging torque, low torque density, poor power factor, and low efficiency. Additionally, the same topology is optimized for reducing the inductances [106].

2) CONSEQUENT POLE

The fundamental design of the consequent pole TFPM machine is delineated in Fig. 20. The stator structure is similar to the conventional TFPM machine, consisting of a ring coil surrounded by U or C-shaped stator core. The rotor contains surface-mounted magnets and laminated iron pole. This machine uses half the number of magnets by generating both PM torque and reluctance torque [107]. However, this topology suffers from high saturation and losses [108].

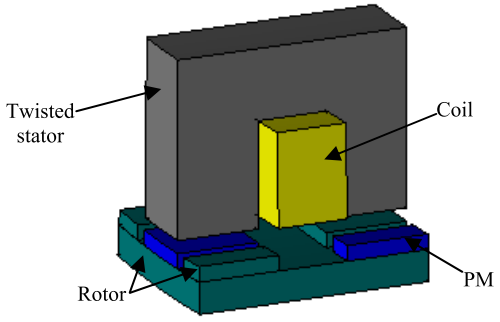

FIGURE 20. Consequent pole TFPM machine.

A consequent pole TFPM machine with a conventional stator placed over ring winding is presented in [109]. The rotor has two ring cores with slots, I-shaped cores fitted in these slots, and PMs settled on the alternate I-shaped cores. The proposed consequent pole machine generates higher torque for the same current with less magnet volume compared to the conventional TFPM machine. Additionally, the consequent pole TFPM machine with improved magnet utilization for low-speed application is developed in [110]. The radially magnetized PMs are mounted on the surface of the middle teeth in the E-shaped stator core. The ring-shaped armature coils are arranged in the upper and lower stator slots, respectively. The FEM simulation results reveal that the consequent pole has 59% higher torque/PM volume with 92% less cogging torque compared to the traditional TFPM machine. However, the shifting of PMs from the rotor to the stator is responsible for 37% lower torque per machine volume.

V. ASSESSMENT OF TFPM MACHINE

Theoretically, the TFPM machine is known for its high torque density, the power rating of the machine can be increased by increasing the pole number. Apart from this, there are other advantages and disadvantages of the TFPM machine which are illustrated as follows:

A. POLE NUMBER AND HIGH TORQUE DENSITY

The main and evident benefit of the TFPM machine is its ability to yield high torque density. The force density of PM machines can be estimated by [69]:

$$\sigma = \alpha_i A B_o \tag{4}$$

where α_i represents the degree of coverage of the PM, A is the current loading, and B_o is the air gap flux density at no-load condition. For a single-sided TFPM machine the current loading and the air gap flux density can be written as [69]:

$$A = \frac{\theta}{2\tau} \tag{5}$$

$$B_o = \frac{B_r}{1 + \frac{g}{h_M}} \tag{6}$$

With θ being the armature current, τ is the pole pitch B_r is the remanence induction of the PM, h_M represents the magnet thickness, and g is the air gap length. This implies that the electrical loading can be increased by simply increasing the number of pole pairs, without changing the armature ampere-turns and the machine diameter. This effect is used by the TFPM machine to achieve high specific torque density. In other words, the TFPM machine has an electric circuit that is decoupled from the magnetic circuit. For a given machine geometry, current and magnetic loading, the homopolar flux path in the stator core permits for the rise in the VA rating of the machine by increasing the number of poles. The increment in the pole number reduces the pole pitch. If leakage is neglected, the amount of flux linked with the stator coil remains the same while the rate of change of flux increases. Therefore, the EMF of the machine at the same mechanical speed increases with the pole number as shown in equation (7) [111]. However, the pole pitch has a lower bound as it affects the power factor and mechanical rigidity of the iron cores [14].

$$E = k_f N \phi \frac{\Omega}{2\tau} \tag{7}$$

where E represents the EMF, k_f is the waveform factor, N is the number of turns, Φ is the flux encircling the winding, ω is the mechanical angular speed of the mover and τ is the pole pitch. The impact of pole number on EMF, torque density, and power factor is examined by various researchers [74], [85], and [102].

A high pole number generates high EMF, torque, and torque density with a low power factor as shown in Fig. 21 (a-b). Moreover, the high pole number degrades the efficiency of the machine by increasing the core losses [94]. Therefore, it is mandatory to choose the optimal pole number for the best performance of the machine for a specific application.

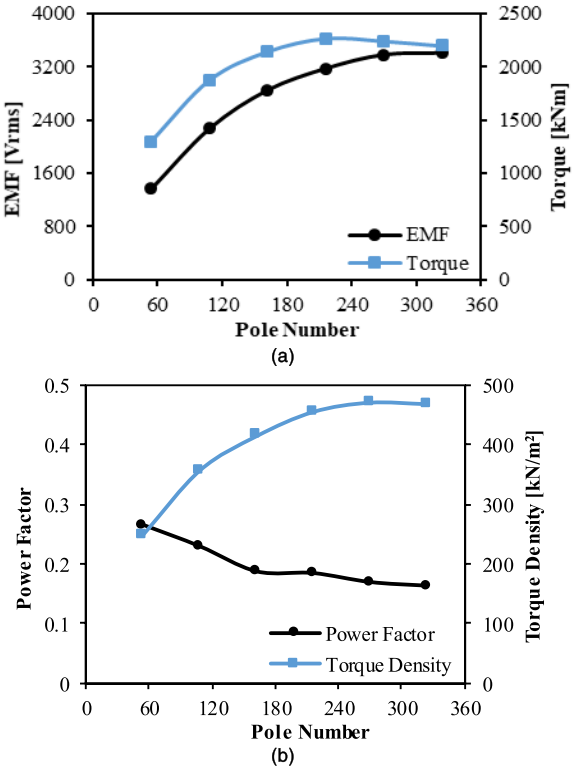

FIGURE 21. Significance of pole number in TFPM machine. (a) EMF and torque. (b) Power factor and torque density.

B. SEPARATE ELECTRICAL AND MAGNETIC LOADING

The average output torque of an electrical machine can be enhanced either by increasing the current loading or increasing the air gap flux density. The increment in the current loading demands a larger winding slot area for keeping the same current density based on the thermal requirement. The higher air gap flux density leads to wider teeth in order to avoid an excessive level of saturation in the iron core. The high torque density in the conventional RFPM machine is bounded by the solid rivalry for the same space between armature winding and stator teeth [111]. However, in the TFPM machine the magnetic and current loadings can be set separately. The magnetic loading is set by the magnet size and stator cores in the circumferential direction, while the MMF is set by the width of the coils in the axial direction. This phenomenon supports a more favorable construction, as the armature winding and the rotor magnetic circuit does not contest for the same available space [63].

C. MULTIPHASE AND FAULT TOLERANCE

Basically, the TFPM machine is a single-phase structural unit. The multiphase structure is produced by axially stacking the single-phase machines as shown in Fig. 22.

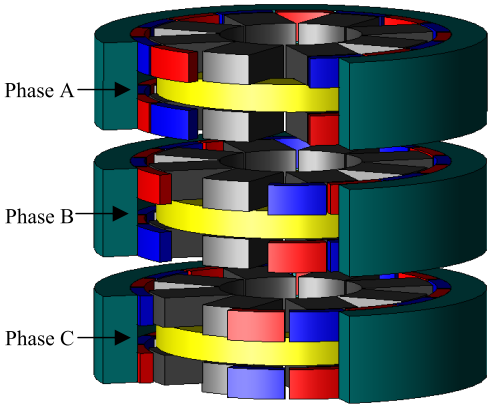

FIGURE 22. Layout of three-phase TFPM machine.

In case of a three-phase machine, the common rotating field is produced by inserting a phase of 120° electrical degrees between three independent alternate fields. This electrical phase shift is created either by mechanically displacing the rotor magnets or stator. The advantage of shifting the PMs rather than stator segments is that the stator segments can be joined together, thus reducing the number of separate parts and consequently the complexity of the production. The entire machine inherits the electromagnetic properties of a single-phase unit. However, the interaction between phases may lead to leakage which causes asymmetry in induced voltages and torque. A fault in one phase does not bring the operation of the machine to a standstill. There will be less torque and more torque ripple [70], [111].

D. END WINDING

The decoupling between the magnetic and electrical circuits allows the usage of a coil with a larger cross-section and suitable slot shape for the reduction of slot leakage in the TFPM machine. For rectangular slots, a square-shaped toroidal winding leads to the lowest copper loss with minimum slot leakage [112]. In comparison with the traditional RFPM machine, one might say that there is no end winding. However, 50% of the winding is active at a specific time in a conventional TFPM machine. This is because of winding between two stator cores is exposed to air instead of iron which aggravates the cooling in the machine. Moreover, these pieces of winding are responsible for leakage, resistive losses, and extra weight [70]. The flux from unutilized magnets will interact with leakage flux which encircles the inactive

winding. The flux orientation in the inactive winding would be similar to flux in the stator. However, the flux orientation of the magnet is in the opposite direction compared with torque production magnets under the stator teeth. Therefore, their interaction may cause a braking torque [111]. Apart from this, the gap created by the winding exposed to air can be utilized for cooling purpose.

E. AIR GAP

The air gap length has been treated as an essential element in the design procedure of electrical machines. The smaller air gap increases the main flux by providing a low reluctance path with improved performance. However, it comes with a trade-off in terms of manufacturing tolerance and high precision machining [74]. With a rotor with surface-mounted magnets, using a large air gap is not so detrimental. This is because the magnets appear as an additional air gap for the stator flux, so the effective air gap that the stator flux has to pass is the sum of the mechanical air gap and the radial magnet length. With flux concentration, it is more important to have a small air gap. The air gap length in most of the conventional generators is usually fixed as [113]:

$$g = \frac{M_{OD}}{1000} \tag{8}$$

where g is air gap length while M_{OD} is the machine's outer diameter. The air gap length plays an influential role in various aspects of the TFPM machine. The air gap length has been thoroughly investigated in various research works [85], [94]. For two different power levels, the relationship of EMF, torque, and power factor with various air gap under fixed diameter, magnetic loading, and copper loss is presented in Fig. 23 (a-c). The decrement in the air gap decreases the reluctance and leakage of the main flux path with a rise in induced voltages by increasing the flux linkage for two different power levels. This higher EMF is responsible for high torque in the TFPM machine. However, the power factor has a different trend for these two power ratings. The kW level TFPM machine shows improvement in power factor at smaller air gaps. The reason behind this enhancement is the small electric loading which overshadows the magnet flux over armature flux. There is no significant advantage that can be obtained for the power factor in MW level TFPM machine.

Additionally, the TFPM machine shows a higher dependency on the air gap compared to the RFPM machine. The air gap below 3 mm should be beneficial for the MW level TFPM machine in terms of mass and cost whereas the threshold for the air gap should be less than 1 mm for kW power rating [114], [115]. Above these thresholds, the TFPM machines scarcely show any benefit compared to traditional RFPM machine. Therefore, it can be concluded that the TFPM machine with a small air gap and a large diameter can be advantageous in terms of mass and cost for wind power applications. However, attention should be given to the mechanical design of such machines as well as the converter requirements.

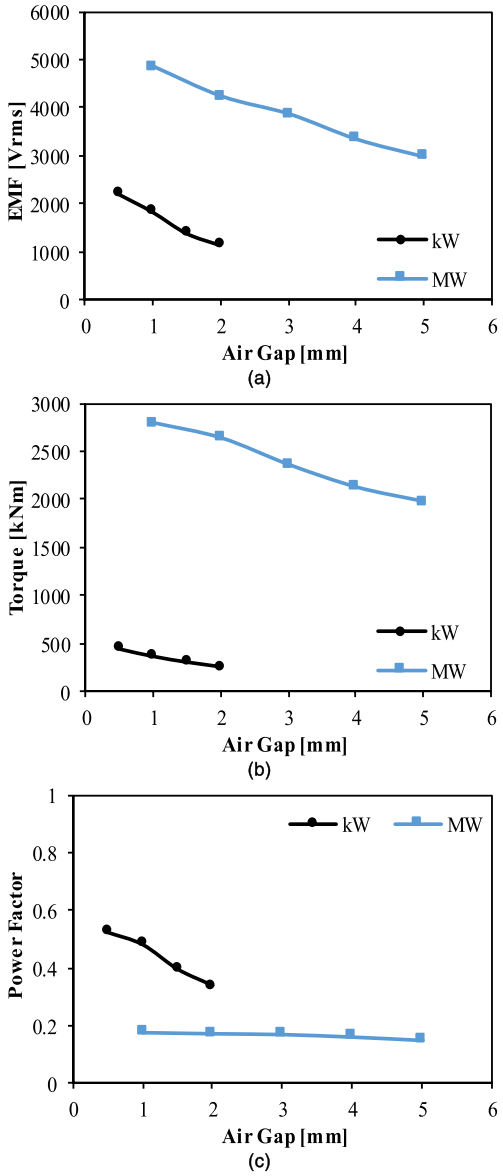

FIGURE 23. Impact of air gap in TFPM machine. (a) EMF. (b) Torque. (c) Power factor.

F. POWER FACTOR

The several advantages of the TFPM machine are met by the disadvantage of low power factor. The typical low power factor in the TFPM machine requires an inverter with a high power-rating which causes two to three-time higher system cost compared to a conventional machine. In normal operation, the working power factor of traditional RFPM and TFPM machine can be calculated by ignoring the phase resistance as [78]:

$$PF = Cos\left(\arctan\frac{IX}{E}\right) \tag{9}$$

where I is the phase current, X is the phase reactance, and E is the back EMF. By neglecting saturation, this ratio can equally be expressed as the ratio of stator peak flux

linkage due to armature current over stator peak flux linkage due to PM flux or flux ratio. This ratio is less than 3 in most TFPM machine compared to 0.3 in traditional RFPM machine. The range of power factor for the TFPM machine lies in between 0.35-0.55 [116]. This low power factor is linked with high armature inductance which leads to high synchronous reactance in the TFPM machine cited by several authors [70]. The segmented structure of the stator core produces a reasonable amount of stator excited flux leakage. The segregated stator core pieces generate flux leakage and fringing between these pieces, which are absent in traditional machines. In [50], values of about 50% magnet leakage flux and about 70% armature flux leakage have been reported. The other reason is the low generation of induced voltage due to improper utilization of PMs in the TFPM machine which causes leakage between adjacent poles. The phenomenon of low induced voltage due to inter-pole flux cancellation is explained in [117]. Furthermore, the saturation dominated by armature flux in the magnetic circuit of the TFPM machine may cause a low power factor [58].

The power factor can be improved by increasing the magnetic loading in the TFPM machine but it will increase the manufacturing cost. The higher utilization of PM volume will also lead to saturation which again causes a low power factor [118]. The selection of pole number is critical because it affects the torque and power factor under fixed magnetic and electrical loadings [55]. Furthermore, the smaller air gap can provide a better power factor by reducing the leakage and improving the effective flux density. However, decreased air gap will challenge the present manufacturing techniques and also mechanical requirements [111]. The power factor is also influenced by the geometrical parameters of the TFPM machine. The impact of the split ratio on the power factor is investigated in [94]. It is observed that a high split ratio is responsible for low power factor in the TFPM machine at fixed electrical and magnetic loadings. The shapes of the magnet and stator tooth have been optimized for high power factor in [97]. The minimization of magnetic flux loss for a better power factor in surface-mounted TFPM is done by utilizing an iron-bridge [119]. The overlapping between stator poles in the claw pole TFPM machine is optimized in [120]. The power factor is improved while maintaining a reasonable torque density. It should be noted that the power factor supposed to be 1 in various research works [62], [68] and [83]. In general, the scope for the improvement of the power factor is limited in the TFPM machine. Therefore, the TFPM machine will only become practically viable until power factors of at least 0.7 can be achieved without sacrificing the high torque density requirement in wind power applications [121].

G. COGGING TORQUE

The cogging torque is an important issue in wind power generators. It creates start-up difficulties and compromises the overall structural integrity of the system by producing noise and mechanical vibration. In the TFPM machine, the stator tooth span is approximately equal to a pole span which generates higher cogging torque [74]. The amount of cogging torque in the TFPM machine can be lowered by designing a machine with higher electrical loading and lower magnetic loading. However, this will lead to poor power factor and higher armature flux leakage [122]. The performance of the machine would be decreased with low air gap flux. Therefore, the best method to reduce this phenomenon is to change the reluctance with respect to the rotor position. The other possibility is to develop a machine whose harmonic sum lowers the peak cogging torque. Furthermore, the slot-pole combination also plays a crucial role in cogging torque minimization where a fractional-pitch winding is unavailable [123].

A variety of methods in literature have been utilized by researchers for the minimization of cogging torque. The common strategy for decreasing the cogging torque in the RFPM machine includes notches, pole width optimisation, and skewing. The concept of magnet skewing and various magnet shapes is explained in [124]. The circular magnets have a high possibility of lessening the cogging torque in the TFPM machine. The core skewing with unequal distribution is discussed in [125]. The skewing is responsible for more than 80% reduction in cogging torque. However, skewing is inefficient because of the detriment in overall machine performance. The effective strategy of stator shifting for diminishing the cogging torque is presented in [126]. The symmetrical and asymmetric shift of the stators in the TFPM machine is discussed in [127], where asymmetric shift has more possibilities to influence the cogging torque waveform. Furthermore, the impact of width and shape of rotor and stator poles on cogging torque is illustrated in [128]. The optimization of stator slot width is carried out for cogging torque in a double C-hoop TFPM machine for wind power applications [129]. The author in [123] presented a design of experiment method for cogging torque reduction. This method is a blend of several techniques such as slot/pole ratio, pole width, stator displacement, and skewing. The 90% of peak cogging torque and 9% average torque is decreased by utilizing this strategy. Apart from this, chamfering, particle swarm optimization and herringbone teeth have been employed for the minimization of cogging torque in TFPM machine [130], [131].

H. MATERIAL CONSIDERATION

This TFPM machine has a complicated 3-D flux pattern and large number of separate small size components, which results in a weak construction and more complex assembly. Therefore, it is necessary to consider suitable material for manufacturing ease with improved performance.

1) IRON CORES

The first pick in materials for the TFPM machine is the material for the iron cores. The selection of iron is based on the permeability of the core and value of magnetic flux density where saturation in the iron occurs. Moreover, the material properties, the thickness of the laminations, and the bonding

of iron powder particles affect the magnetic losses in the rotor and stator cores [78]. The use of SMC for the magnetic core is advantageous for complex geometries with 3-D flux paths. SMC also exhibits lower iron loss because of the tight bonding of iron powder particles at higher frequencies [132]. Besides, SMC has low permeability and saturates at a lower flux density. The advantage of utilizing laminated steel is its cost and higher magnetic properties with lower iron loss at low operating frequency. However, complex 3-D flux paths cannot be accomplished with laminated steel and some trade-offs should be made in either the iron loss or geometry [70].

The SMC and laminated steel have been utilized in the manufacturing process of the TFPM machine for various direct-drive applications. The laminated steel along with SMC has been employed for outer rotor TFPM machines in [133]. Furthermore, the performance comparison of the TFPM machine for wind power applications based on laminated steel and SMC has been presented in [95]. The analysis indicated both machines achieve similar performance with small differences. Thus, both options are still widely considered for designing TFPM machine.

2) PERMANENT MAGNET

The PM selection criteria need special consideration in the design process of the TFPM machine for achieving a high power factor with reasonable torque density. In literature, ferrite magnets and rare earth magnets are employed in the design procedure of the TFPM machine [104], [134]. Because of high energy density, the TFPM machine design often requires rare earth magnets (NdFeB or SmCo) for improvement in magnetic loading which leads to a high power factor. However, these magnets are liable to issues of cost fluctuation in rare earth metals. Whereas, ferrite magnets represent a low-cost alternative for applications with low requirement. Their utilization requires a trade-off between higher magnet volume and lower magnetic flux as a result of much lower energy density (one-tenth of rare earth magnets) [105]. Furthermore, ferrite magnets show a high risk of demagnetization. The performance comparison of the TFPM machine with various magnets is carried out in [95]. The rare earth magnets provide high torque density with a high power factor. Therefore, it is concluded that the rare earth magnet should be used for high torque density TFPM machine designs.

I. LOSSES AND EFFICIENCY

For various applications, the losses are considered for the estimation of operating cost, power rating, and heating without deterioration of the insulation. The efficiency of an electrical machine at normal working conditions is chosen by losses which include iron losses, copper losses, and other losses. The iron losses comprise of hysteresis losses and eddy current losses. Whereas, the copper losses or Ohmic losses are found in windings of the stator. Moreover, three additional losses also present in the electrical machine such as ventilation losses, friction losses, and stray losses. Practically, the friction and ventilation losses have no significant impact on the machine's efficiency for fixed speed. However, stray losses mainly arising from the additional core losses generated in the iron by distortion of the magnetic flux by load current which can be taken as 1% of the overall output power [135].

The high magnetic and electrical loadings of the machine offer a risk for the machine, particularly for the TFPM machine with a high specific torque density. The topologies which generate the highest torque tend to have high pole number. This produces a high fundamental frequency of the magnetic field in the TFPM machine and associated core losses, resulting in a drop in efficiency. Therefore, this machine is more appropriate for medium and low-speed applications where iron lamination is used for the magnetic core [58]. For high operating frequency where eddy current losses are dominant, the SMC formed by compacting and bonding iron powder particles can be beneficial for the magnetic core. These particles are coated with an electrically insulating layer which is responsible for little conduction. The high saturation in TFPM is also responsible for the core losses. The impact of saturation can be lessened by utilizing high-grade steel or grain oriented steel. Additionally, the TFPM machine has lower copper losses due to the short end winding. The winding between two stator cores is surrounded by air which contributes to copper loss and cooling problems in the machine and should be considered as end winding [70].

The loss calculation of claw pole TFPM is presented in [136]. This method is combined with an iron loss calculation model that takes nonlinear effects, saturation, and a bias component in the magnetic flux into consideration. The eddy current losses in non-conventional flux concentrated TFPM machines are investigated through a 3-D transient approach in [137]. The eddy currents on the stator poles and inside the stator core are significant due to the existence of normal magnetic fields. Whereas, the eddy current losses in rotor pole are mainly present at the center of the pole region due to the high concentration of opposing magnetic fields from magnets. Besides, the eddy currents accumulate themselves on the corners of the magnets. The rapid estimation of the eddy current is developed for the TFPM machine through 3-D MEC and 2D FEM [138]. In [102], the optimization process based on a genetic algorithm is developed for three TFPM machines. Various investigation shows that the efficiency of TFPM machine is below 90% [105], [134], and [139]. The research on TFPM machine mainly focused on the design, optimization, and modelling of TFPM machine with very little comprehensive attention to the losses and efficiency of TFPM machine.

VI. MODELLING TECHNIQUES

An overview of the results obtained in literature by the different modelling methods used to calculate the performance of a TFPM machine is given in this section. The modelling methods that have been found in literature used to model the transverse flux machine are: analytical models, MEC, or in majority, FEM.

A. SIZING EQUATIONS

The analytical models commonly utilize the supposition of a sinusoidally varying flux density in the air gap. The first step in analytical models is sizing the machine based on the dimensions where the performance of the machine in terms of induced voltage and force is obtained through PM flux linkage [78]. This is done in 2-D or quasi 3-D. The flux leakage in the axial direction is not considered in the 2-D estimation of the flux density which causes significant error [121]. The impact of design parameters on the performance of the machine is determined through these 2-D models so that the number of 3-D FEM simulations can be reduced [140]. Furthermore, the analytical model based on quasi 3-D uses two cross-sections (plane perpendicular to the axis and additional plane along the axis) of the machine for the calculation of flux leakage in the axial direction. The end effects due to finite iron dimensions are not modelled because iron is assumed to have infinite depth in both planes. The difference between 2-D and quasi 3-D approach for the estimation of flux leakage is 32% [141]. Another way to lessen the number of FEM calculations is to combine numerical and analytical models. The amplitude of flux linkage is achieved from a 3-D FEM model in an aligned position for the estimation of machine performance through voltage based analytical equations. The flux linkage is considered to be sinusoidal or achieved from Fourier series using geometry parameter and FEM simulations of two rotor positions [70].

In traditional sizing equations, the designer needs to choose the magnetic loading, electric loading, and efficiency based on different factors. The machine power in these sizing equations is directly proportional to stack length and square of machine diameter. In general, if stator leakage inductance and winding resistance are neglected, the output power for any electrical machine can be shown as [142]:

$$P_R = \eta \frac{m}{T} \int_0^T e(t)i(t)dt = \eta m K_p E_{pk} I_{pk} \tag{10}$$

where P_R is the rated power, η is the efficiency, m represents the number of phases, $e(t)$ and E_{pk} are the phase EMF and its peak value, K_p is the power waveform factor, $i(t)$ and I_{pk} are the phase current and the peak phase current, T represents the period of one cycle of the EMF. The analytical demonstration of EMF in terms of PM height for double-sided flux concentrated topology is presented in [143]. However, the leakage and saturation have been neglected in the sizing equations. An updated version of sizing equations for the same topology has been illustrated in [92]. The EMF equation of this machine is represented by PM width in the circumferential direction. The author also analytically calculated the winding resistance and leakage in the machine. An outer rotor single-sided TFPM for wind power has been analytically modelled in [59]. The author analytically deduces the equations for EMF, leakage, and fringing. Furthermore, the general purpose torque sizing equation and the power factor of the machine are calculated in [144]. The author defined the equation of power factor in terms of self and leakage inductances.

B. MAGNETIC EQUIVALENT CIRCIUT

The MEC is constructed from elements that model the different flux paths and flux sources in the machine. The flux paths in the machine are restricted to predefined elements or ''flux tubes'' with a constant flux density. The flux through these tubes is dictated by dividing the MMF over the tube by the reluctance of the tube. The flux distribution in the machine is achieved by explaining the system of equations illustrating the developed MEC of flux tubes and MMF sources. However, the precise depiction of the flux paths with flux tubes is specific for each machine geometry. The variation in geometrical parameters may bring a change in flux distribution which requires a new reluctance network. Besides, the development of such reluctance requires the pre-knowledge of the flux paths in the machine [145].

After the preliminary sizing process, a more comprehensive examination is carried out using MEC. A MEC of the TFPM machine can be developed in 2-D or 3-D. The 2-D MEC is not generally employed because it does not include flux leakage which leads to an inaccurate solution. The 3-D MEC models can achieve an accuracy of 70 to 90% for fixed geometries [70]. The accuracy of the MEC models varies with rotor position. The aligned rotor position is responsible for a 10% error while an unaligned position causes a 30% error. Several MEC models for the TFPM machine have been developed in literature [63], [82], and [146]. The MEC composed of magnetic charge and magnetic imaging technique for the representation of magnetic flux distribution within the air gap of a TFPM machine is presented in [147]. The calculated result is within 15% accuracy compared to the experimental result. The results of the suggested MEC is in a reasonable agreement with those by 3-D FEM, while the calculation time of the proposed method is reduced to about 1/3. The improved MEC for flux concentrated TFPM machine is developed in [148]. The model consists of a series-parallel combination of flux tubes with an average error of less than 7% between simulated and experimental data [149]. The double-sided flux concentrated TFPM machine with a quasi-U-shaped stator is modelled through MEC in [150]. The 2-D MEC estimates the complex 3-D flux path with the inclusion of magnetic saturation. The model is capable of adapting any geometry with a 5% error and 25 times improvement in computational time. Furthermore, the MEC of TFPM machine is developed through a complex permeance method for minimization of calculation time is presented in [151].

C. FINITE ELEMENT METHOD

The most commonly utilized numerical modelling technique is the FEM. The 2-D and 3-D models can be used to demonstrate the performance of the TFPM machine. The 2-D investigation is carried out in various research works [152], [153]. In [154], it is illustrated that an error of 10% in results is obtained through efforts compared to 3-D FEM. The other

works found to be unsuitable with a deviation of 50% in results [70]. The 3-D FEM has a much smaller deviation which predicts the performance accurately [155]. Therefore, 3-D is normally employed as a design tool for TFPM regardless of the fact that is a time-consuming method.

VII. SCALIBILITY

The direct-drive PM generator system is an attractive option in wind power applications because of various advantages compared to the traditional geared concept. However, the low-speed operation of the direct-drive PM generator is responsible for the increase in diameter, weight, and cost of the generator. The inverse relationship of rated power level and rotor speed also causes technical difficulty of transport and assembly. Therefore, the cost of energy production from direct-drive PM generators can be reduced by analyzing the fundamental factor of scaling [156]. The scaling laws quickly evaluate the effect of variation machine size for a new design. These laws also reduce the calculation time for FEM simulation and other number numerical methods [157].

For producing high torque in direct-drive PM generators it requires extra PM volume, conducting material, and iron, which leads to an increase in cost [22]. The type of power converter is strongly dependent on the machine synchronous reactance. The reactance above 1.5 p.u. requires a high rating of the power converter. The expenditure of active material in generator increase with higher power rating while there is an increment in power converters cost for lower power ratings [158]. A comparative study has been carried out for conventional RFPM machine and single-sided surface-mounted TFPM machine at two different power ratings [115]. The TFPM machine performs better compared to the RFPM machine at a low power level with high average torque as depicted in Fig. 24 (a) & (b). The kW TFPM machine has a favorable power factor of 0.34 compared to 0.15 in the MW power level. This is mainly due to the low electrical loading, smaller air gap length, and less saturation. Furthermore, the low power TFPM machine has improved the power factor than the high power TFPM machine. The high power TFPM machine, the performance is strongly dependent on air gap length [114]. Thus, the comprehensive study of the TFPM machine is incomplete without analyzing the impact of scaling on the performance of the TFPM machine.

VIII. POWER ELECTRONICS AND CONTROL

The operation of the TFPM machine is similar to the conventional PM synchronous machine allowing similar control strategies and power electronic converters [161]. This section mainly deals with control techniques and power converters employed in PM based transverse flux machines.

A. CONTROL STRATEGY

The overall control of the wind energy conversion system (WECS) is the most significant factor for the effective generation of electric power from wind energy. The control schemes are applied in various parts and subsystems of WECS.

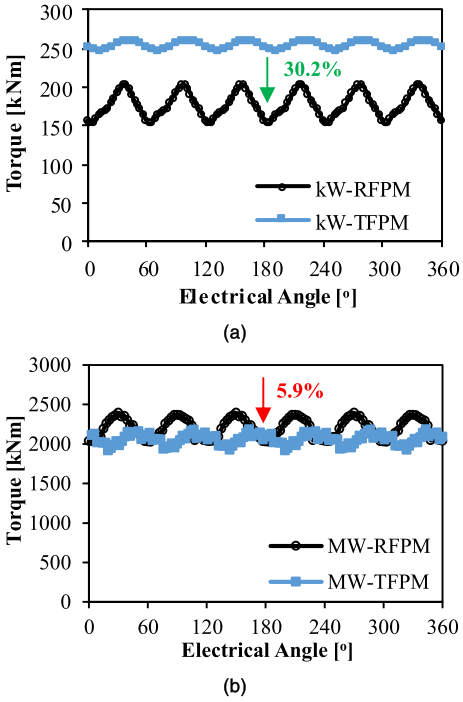

FIGURE 24. Torque comparison under two different power levels. (a) kW power level. (b) MW power level.

There are three basic subsystems that constitute the WECS control system [162]. This subsection concentrates on machine side control (MSC) of WECS.

- Turbine control (e.g., pitch control for aerodynamic);
- Machine (generator) side control;
- Grid side control.

The variable-speed operation and maximum capture of energy are controlled by turbine controller and MSC. The MSC is responsible for the power delivery from the generator to the grid. The MSC method also aims at the decoupling of torque and flux. The MSC is divided into two commonly used strategies i.e. field oriented control (FOC) and direct torque control (DTC). The performance comparison of two methods has been carried out in various research works [163], [164]. Both control methods have similar dynamic responses and each of them allows the active and reactive current components (either torque or flux) of the machine to be controlled independently. The FOC is a mature technique and commonly employed in the industry despite of better dynamic response from DTC. A tabular comparison FOC and DTC is done in Table 2.

1) FIELD ORIENTED CONTROL

For generator speed, and/or power and voltage control, the FOC comprises of a dual loop (internal and external loops) control technique. The external loop control demands the generation of a representative three-phase reference current. The internal loop control is typically based on a synchronous reference frame or a natural reference frame [165].

TABLE 5. Comparison Between FOC and DTC.

Parameters	FOC	DTC
Coordinate transformation	Yes	No
Rotor position	Precisely	Approximately
Coupling between D and Q	Poor	Better
Parameter sensitivity	Poor	Better
Torque and harmonic ripple	Low	High
Dynamic response	Poor	Better
Current protection	Better	Poor
Digital signal processing	More	Less

The maximum electromagnetic torque is usually achieved with minimum stator current when the d-axis of the stator current is set to zero and developed torque is controlled by the q-axis of the stator current. Since the FOC directly controls the current, the total line current is used for torque generation, which tends to increase the machine's optimal efficiency [166], [167]. The capability of independent d-axis current control may be particular suitable for power factor correction in the TFPM machines.

A system-level six sigma robust optimization is presented for designing a drive system with TFPM machine and FOC [168]. The optimal solution provides a 5.1% increment in output power with better reliability and low cost. Additionally, the control parameters are not sensitive to variation of motor parameters. The claw pole type three-phase TFPM machine with FEM calculation and experimental results is presented for robotic applications [169]. The dq-axis inductances for the controller design of a FOC are obtained from the parameter identification scheme. The simulated and measured torques are compared, and the maximum torque per ampere curve with efficiency and power factor map are shown for the given prototype. Moreover, the Matlab model for the TFPM machine is developed for enabling the fast simulation (4.2 million times) with power converters and other components in [170]. The model is tested with a FOC and compared to conventional FEM simulations.

2) DIRECT TORQUE CONTROL

In direct control strategies, torque and power are estimated and directly controlled, resulting in less complex and faster algorithms. The use of the DTC method eliminates internal control loops and transformation between reference frames. In a typical implementation, the outputs of the hysteresis comparator and flux angle are directly used for generating the switching pulses for the converter. The performance of the generator side control technique is evaluated by ripples in current and torque [162], [171].

To reduce torque ripple and obtain faster torque response, a DTC with a position sensor instead of a flux linkage observer has been employed for the TFPM machine with brushless DC drive [172]. The phase advance commutation has been inserted in the foregoing DTC which achieves a much larger torque per ampere. The improvement of system response speed with reduced pulsation of torque in the TFPM machine is brought by an improved scheme of fuzzy DTC [173]. The simulated results showed that the fuzzy DTC scheme has better accuracy than conventional DTC.

B. POWER ELECTRONIC CONVERTERS

Theoretically, the TFPM machine is known for its high torque density compared to traditional PM machines. This torque density is beneficial for dire-drive wind power applications as it leads to reduced machine size, mass, and cost. However, poor power factor associated with the TFPM machine has a negative impact on the power electronic converter size, cost, and efficiency. The PM machine with poor power factor such as Vernier and TFPM machine can increase the cost of power converter by 50% approximately [174]. Furthermore, it is worth noting that the power factor has a considerable impact on the machine side converter rating because the grid side converter is unaffected by the generator power factor. At the same time, the huge size of the direct-drive generator will significantly contribute to the overall mass and cost of the direct-drive powertrain system [175]. Any reduction in size or mass of generator and converter active materials due to higher torque production capability of TFPM machine is going to be beneficial for system-level performance.

The existing research for TFPM machines is largely limited to design, modelling, and optimization. Therefore, power converter topologies employed for direct-drive conventional PMSG can be used for the TFPM machine because of similar operation. In recent decades, different converter topologies have been investigated of WECS and it is not possible to classify all the converters based on one parameter/operations. The power converter topologies are divided into four different groups in Fig. 25. Additionally, the operating principle of these power converter topologies with promising features and drawbacks are discussed in this sub-section.

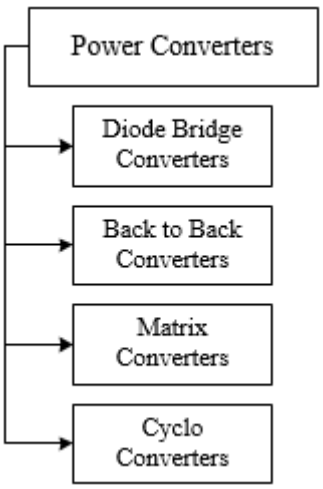

FIGURE 25. Classification of power converters.

1) DIODE BRIDGE CONVERTERS

In this converter design, the power flow is unidirectional, i.e. from the generator to the grid. The variable frequency and magnitude alternating current (AC) power from the wind turbine generator is initially transformed into a DC power by a diode rectifier and then reconverted into AC power at different frequency and voltage level by a controlled inverter. The diode bridge rectifier is cost-effective, reliable, and simple to implement [176]. However, this topology has the drawback of large harmonic distortion which affects the performance of the utility system [177]. Another potential issue is the inability of power factor control on the machine side. Additionally, this converter concept has been practically implemented by Clipper Liberty, Gold Wind, and Vensys.

2) BACK TO BACK CONVERTERS

The back to back (BTB) converter is identical on both the generator and grid side and connected via DC-link. It consists of two typical pulse width modulated (PWM) voltage source inverter (VSI). The grid side converter enables to control the active and reactive power flow to the grid, enhancing the output power quality by lessening total harmonic distortion (THD). The generator side converter works as a driver, controlling the magnetization demand and the required rotor speed or power of the generator. The independent control capability of the two converters is provided by the decoupling capacitor between the grid side and generator side converter, and the DC link voltage is maintained from either the grid or generator side. The BTB converters are classified as low voltage and medium voltage converters. This converter topology is quite dominating in wind applications and employed by Vestas, Siemens, GE energy. Furthermore, a summary of the merits and demerits are presented as below [177], [178]:

Merits:

- Power flow is bidirectional;
- Generator is full decoupled from grid, excellent fault ride through ride (FRT) compliance;
- Full control of the grid and generator current.

Demerits:

- High cost and low efficiency;
- The DC component link can be a weak link in the BTB system.

3) MATRIX CONVERTERS

The matrix converter is a unique design of AC to AC conversion without any intermediate DC-links, leading to more silicon-based conversion. The converter comprises of an array of bidirectional switches placed at the interaction points of input and output phases. The output is regulated by the selective closing and opening of the switches. A filter on the input side assists commutation and restricts the switching generated harmonics from propagating the power input. The matrix converter is typified into direct matric converter and multi-modular matrix converter. Moreover, the merits and demerits of this topology are summarized as [178], [179]:

Merits:

- Low cost, compact and reliable design due to absence of DC-link capacitors;
- Low thermal stresses and switching losses.

Demerits:

- Low voltage gain requires bidirectional switches;
- Complex commutation control and modulation techniques;
- Complicated FRT compliance.

4) CYCLO CONVERTERS

The cyclo converter performs AC to AC conversion without utilizing intermediate DC-link similar to the matrix converter. It is also known as a frequency converter, and has the reputation of very robust. This technique may be applicable if the generator fundamental frequency is lower than 1/3 of the grid frequency, though the high level of harmonic and the inability of harmonic control and power factor control may be the concerns. The merits and demerits of this topology are summarised as [177]:

Merits:

- Lower conduction and commutation losses;
- Compact design with bidirectional power flow.

Demerits:

- Complex control and poor input power factor;
- Low voltage transfer ratio.

IX. CONCLUSION

The review in this paper presents a summary of the state of art and guidelines for future research in the TFPM machines. The literature on various design categories of TFPM machine is presented with the working principle. The TFPM machine is characterized by high pole number, modularity, fault-tolerant capability, air gap length, and efficiency. The analysis of power factor and cogging torque, the selection of air gap, and material, modelling techniques and scaling effects are also considered in this paper. Based on available literature, the control methodology and power converter topologies are also discussed in this paper. Furthermore, the advantages and weakness of typical wind turbine systems available in the market are examined along with direct-drive PM generators. There is always a scope for improving the existing research. The following recommendations will further reform the research work related to the TFPM machine:

- Scaling effect in TFPM and RFPM machine.
- Detailed analysis of losses and efficiency in TFPM machine.
- Effect of demagnetization in TFPM machine.
- Noise and vibration in TFPM machine.
- Investigation of aspect ratio in TFPM machines.
- Development of controller topology for TFPM machine.
- System level investigation and optimization of TFPM machine

REFERENCES

[1] W. Tong, "Fundamentals of wind energy," *WIT Trans. State-of-the-art Sci. Eng.*, vol. 44, pp. 1–48, Apr. 2010.

[2] S. Dawn, P. K. Tiwari, A. K. Goswami, A. K. Singh, and R. Panda, "Wind power: Existing status, achievements and government's initiative towards renewable power dominating india," *Energy Strategy Rev.*, vol. 23, pp. 178–199, Jan. 2019.

[3] A. D. Hansen and L. H. Hansen, "Wind turbine concept market penetration over 10 years (1995–2004)," *Wind Energy*, vol. 10, no. 1, pp. 81–97, 2007.

[4] X. Yang, D. Patterson, and J. Hudgins, "Permanent magnet generator design and control for large wind turbines," in *Proc. IEEE Power Electron. Mach. Wind Appl.*, Jul. 2012, pp. 1–5.

[5] F. Blaabjerg, Z. Chen, and S. B. Kjaer, "Power electronics as efficient interface in dispersed power generation systems," *IEEE Trans. Power Electron.*, vol. 19, no. 5, pp. 1184–1194, Sep. 2004.

[6] R. Todd, M. Barnes, and A. C. Smith, "Design study of doubly-fed induction generators for a 2MW wind turbine," *Wind Eng.*, vol. 33, no. 5, pp. 497–507, Oct. 2009.

[7] H. A. Hoseynabadi, P. J. Tavner, and H. Oraee, "Reliability comparison of direct-drive and geared drive wind turbine concepts," *Wind Energy*, vol. 13, no. 1, pp. 62–73, 2010.

[8] R. S. Semken, M. Polikarpova, P. Roytta, J. Alexandrova, J. Pyrhonen, J. Nerg, A. Mikkola, and J. Backman, "Direct-drive permanent magnet generators for high-power wind turbines: Benefits and limiting factors," *IET Renew. Power Generat.*, vol. 6, no. 1, pp. 1–8, Jan. 2012.

[9] S. Siegfriedsen and G. Böhmeke, "Multibrid technology—A significant step to multi-megawatt wind turbines," *Wind Energy*, vol. 1, no. 2, pp. 89–100, Dec. 1998.

[10] S. Ma, X. Zhang, Q. Du, L. Shi, and X. Meng, "Optimization design of a new type of interior permanent magnet generator for electric vehicle range extender," *J. Electr. Comput. Eng.*, vol. 2019, pp. 1–10, May 2019.

[11] R. Rashmi, V. Ramanujan, and M. Purushotham, "Permanent magnet synchronous generator configuration in wind turbines - technological status review, survey and market trends," *Int. J. Eng. Res.*, vol. 6, no. 2, pp. 23–31, 2015.

[12] P. J. Sola, "Advanced structural modelling and design of wind turbine electrical generators," Ph.D. dissertation, Dept. Electron. Elect. Eng., Strathclyde Univ., Glasgow, Scotland, 2016.

[13] A. Grauers, "Design of direct-driven permanent magnet generators for wind turbines," Ph.D. dissertation, School Elect. Comput. Eng., Chalmers Univ. Tech., Goteburg, Sweden, 1996.

[14] M. A. Waqas, "A low-leakage linear transversal-flux machine for a free-piston generator," Ph.D dissertation, Dept. Elect. Syst., KTH Roy. Inst. Tech., Stockholm, Sweden, 2003.

[15] B. Zhang, T. Epskamp, M. Doppelbauer, and M. Gregor, "A comparison of the transverse, axial and radial flux PM synchronous motors for electric vehicle," in *Proc. IEEE Int. Electr. Vehicle Conf. (IEVC)*, Dec. 2014, pp. 1–6.

[16] G. Q. Bao and J. Z. Jiang, "A new transverse flux permanent motor for direct drive application," in *Proc. IEEE Int. Conf. Electric Mach. Drives*, May 2005, pp. 1192–1195.

[17] H. Vihriälä, "Control of variable speed wind turbines," Ph.D. dissertation, Dept. Elect. Eng., Tampere Univ. Tech., Hervanta, Finland, 2002.

[18] A. D. Hansen, F. Iov, F. Blaabjerg, and L. H. Hansen, "Review of contemporary wind turbine concepts and their market penetration," *Wind Eng.*, vol. 28, no. 3, pp. 247–263, May 2004.

[19] L. H. Hansen, L. Helle, F. Blaabjerg, E. Ritchie, S. M. Nielsen, H. W. Binder, P. E. Sorensen, P. Enjar and B. Sorensen, "Conceptual survey of generators and power electronics for wind turbines," Riso Natl. Lab., Roskilde, Denmark, Tech. Rep. Riso-R-1205(EN), Dec. 2001.

[20] H. Polinder and J. Morren, *Developments in Wind Turbine Generator Systems*. Hammamet, Tunisia: Electrimacs, 2005.

[21] H. Polinder, F. F. A. Van Der Pijl, G.-J. De Vilder, and P. J. Tavner, "Comparison of direct-drive and geared generator concepts for wind turbines," *IEEE Trans. Energy Convers.*, vol. 21, no. 3, pp. 725–733, Sep. 2006.

[22] M. R. Dubios, H. Polinder and J. A. Ferriera, "Comparison of generator topologies for direct-drive wind turbine," in *Proc. Nordic Countries Power Ind. Electron. Conf.*, Aalborg, Denmark, Jun. 2000, pp. 22–26.

[23] J. Sonsen, "Impact of wind energy in a future," Ph.D. dissertation, Dept. Elect. Eng., KU Leuven, Leuven, Belgium, Dec. 2005.

[24] A. Ramkumar, "Performance analysis of doubly fed induction generator based wind energy conversion systems," Ph.D. dissertaiton, Dept. Elect. Electron. Eng., Kalasalingam Univ., Krishnankoil, India, Jun. 2014.

[25] D.-J. Bang, H. Polinder, G. Shrestha, and J. A. Ferreira, "Promising direct-drive generator system for large wind turbines," in *Proc. Wind Power Grid EPE Wind Energy Chapter 1st Seminar*, Mar. 2008, pp. 1–10.

[26] J. R. Hendershot and T. J. E. Miller, "Sizing & computer-aided design," in *Design of Brushless Permanent-Magnet Motors, Magna Physics Publishing*. Oxford, U.K.: Clarendon Press, 1994, ch. 12, sec. 12.2, pp. 12-2–12-5.

[27] J. Ribrant and L. Margareta Bertling, "Survey of failures in wind power systems with focus on swedish wind power plants during 1997–2005," *IEEE Trans. Energy Convers.*, vol. 22, no. 1, pp. 167–173, Mar. 2007.

[28] A. Marx, "An in-depth comparative study of direct-drive versus gearbox wind turbines," M.S. thesis, School Ind. Eng. Manage., KTH Roy. Inst. Tech., Stockholm, Sweden, Nov. 2018.

[29] G. Bywaters, V. John, J. Lynch, P. Matilla, G. Norton and J. Stowell, "Northern power systems windPACT drive train alternative design study report," Nat. Renew. Energy Lab., Golden, CO, USA, Tech. Rep. NREL/SR-500–35524, Oct. 2004.

[30] S. Heier, *Grid Integration of Wind Energy Conversion Systems*. Hoboken, NJ, USA: Wiley, 1999.

[31] F. Zhang, H. Wang, G. Jia, D. Ma, and M. G. Jovanovic, "Effects of design parameters on performance of brushless electrically excited synchronous reluctance generator," *IEEE Trans. Ind. Electron.*, vol. 65, no. 11, pp. 9179–9189, Nov. 2018.

[32] Z. Q. Zhu and J. Hu, "Electrical machines and power-electronic systems for high-power wind energy generation applications," *Compel-Int. J. Comput. Math. Electr., Electron. Eng.*, vol. 32, no. 1, pp. 7–33, 2013.

[33] J. Chen, C. V. Nayar, and L. Xu, "Design and finite-element analysis of an outer-rotor permanent-magnet generator for directly coupled wind turbines," *IEEE Trans. Magn.*, vol. 36, no. 5, pp. 3802–3809, Sep. 2000.

[34] Y. Chen, P. Pillay, and A. Khan, "PM wind generator topologies," *IEEE Trans. Ind. Appl.*, vol. 41, no. 6, pp. 1619–1626, Nov. 2005.

[35] F. Libert, "Design, optimization and comparison of permanent magnet motors for a low-speed direct-driven mixer," Ph.D. dissertation, Dept. Elect. Eng., KTH Roy. Inst. Tech., Stockholm, Sweden, 2004.

[36] H. Li and Z. Chen, "Overview of different wind generator systems and their comparisons," *IET Renew. Power Gener.*, vol. 2, no. 2, pp. 123–138, Jun. 2008.

[37] M. R. Dubios, "Review of electromechanical conversion in wind turbines," Delft Univ. Technol., Delft, The Netherlands, Tech. Rep. EPP00.R03, Apr. 2000.

[38] A. McDonald and N. A. Bhuiyan, "On the optimization of generators for offshore direct drive wind turbines," *IEEE Trans. Energy Convers.*, vol. 32, no. 1, pp. 348–358, Mar. 2017.

[39] R. D. Paiva Jr, V. C. Silva, S. I. Nabeta, and I. E. Chabu, "Magnetic topology with axial flux concentration: A technique to improve permanent-magnet motor performance," *J. Microw., Optoelectron. Electromagn. Appl.*, vol. 16, no. 4, pp. 881–899, Dec. 2017.

[40] F. Libert and J. Soulard, "Design study of different direct-driven permanent-magnet motors for a low speed application," in *Proc. Nordic Wksp. Power Ind. Electron.*, Trondheim, Norway, Jun. 2004, pp. 1–6.

[41] A. Parviainen, "Design of axial-flux permanent-magnet low-speed machines and performance comparison between radial-flux and axial-flux machines," Ph.D. dissertation, Dept. Elect. Eng., Lappeenranta Univ. Tech., Lappeenranta, Finland, 2005.

[42] S. Kahourzade, A. Mahmoudi, H. W. Ping, and M. N. Uddin, "A comprehensive review of axial-flux permanent-magnet machines," *Can. J. Electr. Comput. Eng.*, vol. 37, no. 1, pp. 19–33, 2014.

[43] P. Lampola, "Directly driven, low-speed permanent magnet generators for wind power applications," Ph.D. dissertation, Dept. Elect. Commun. Eng., Helsinki Univ. Tech., Helsinki, Finland, 2000.

[44] S. Huang, M. Aydin, and T. A. Lipo, "TORUS concept machines: Pre-prototyping design assessment for two major topologies," in *Proc. Conf. Rec. IEEE Ind. Appl. Conf. 36th IAS Annu. Meeting*, Sep. 2001, pp. 1619–1625.

[45] B. J. Chalmers and E. Spooner, "An axial-flux permanent-magnet generator for a gearless wind energy system," *IEEE Trans. Energy Convers.*, vol. 14, no. 2, pp. 251–257, Jun. 1999.

[46] A. Parviainen, "Design of axial-flux permanent magnet low-speed machines and performance comparison between radial-flux and axial-flux machines," Ph.D. dissertation, Dept. Elect. Eng., LUT Univ., Lappeenranta, Finland, 2005.

[47] D. Vizireanu, X. Kestelyn, S. Brisset, P. Brochet, Y. Milet, and D. Laloy, "Polyphased modular direct-drive wind turbine generator," in *Proc. Eur. Conf. Power Electron. Appl.*, Sep. 2005, p. 9.
[48] D. Vizireanu, S. Brisset, and P. Brochet, "Design and optimization of a 9-phase axial-flux PM synchronous generator with concentrated winding for direct-drive wind turbine," in *Proc. Conf. Rec. IEEE Ind. Appl. Conf. 41st IAS Annu. Meeting*, Oct. 2006, pp. 1912–1918.
[49] Z. Zhang, R. Nilssen, S. M. Muyeen, A. Nysveen, and A. Al-Durra, "Design optimization of ironless multi-stage axial-flux permanent magnet generators for offshore wind turbines," *Eng. Optim.*, vol. 49, no. 5, pp. 815–827, May 2017.
[50] A. Cosic, "Analysis of a novel transverse flux machine with a tubular cross-section for free piston energy converter application," Ph.D. dissertation, School Elect. Eng., KTH Roy. Inst. Tech., Stockholm, Sweden, 2010.
[51] P. Zheng, B. Yu, H. Yan, Y. Sui, J. Bai, and P. Wang, "Electromagnetic analysis of a novel cylindrical transverse-flux permanent-magnet linear machine," *ACES J.*, vol. 28, no. 9, pp. 879–891, Sep. 2013.
[52] J. Luo, B. Kou, H. Zhang, and R. Qu, "Development of a consequent pole transverse flux permanent magnet linear machine with passive secondary structure," *CES Trans. Electr. Mach. Syst.*, vol. 3, no. 1, pp. 39–44, Mar. 2019.
[53] J. Wang, K. T. Chau, J. Z. Jiang, and C. Yu, "Design and analysis of a transverse flux permanent-magnet machine using three-dimensional scalar magnetic potential finite element method," *J. Appl. Phys.*, vol. 103, no. 7, pp. 1–3, Oct. 2007.
[54] Y. Guo, J. Zhu, H. Lu, and J. Jin, "Parameter computation and performance prediction of a claw pole/transverse flux motor with soft magnetic composite core," *J. Sci. Tech. Eng., vo.*, vol. 1, no. 1, pp. 13–16, Jun. 2007.
[55] S. Baserrah, "Theoretical and experimental investigations of a permanent magnet excited transverse flux machine with a segmented stator for in-wheel motor applications," Ph.D. dissertation, Dept. Phys. Elect. Eng., Bremen. Univ., Bremen, Germany, 2014.
[56] B. E. Hasubek, "Analysis and design of passive rotor transverse flux machine with permanent magnet on the stator," Ph.D. dissertation, Dept. Elect. Comput. Eng., Calgary Univ., Calgary, AT, Canada, 2000.
[57] M. R. Harris and B. C. Mecrow, "Variable reluctance permanent magnet motors for high specific output," in *Proc. 6th Int. Conf. Electr., Machi. Drives Conf. Publ.*, Oxford, U.K., Sep. 1993, pp. 437–442.
[58] M. R. Harris, G. H. Pajooman, and S. M. A. Sharkh, "Performance and design optimisation of electric motors with heteropolar surface magnets and homopolar windings," *IEE Proc. Electr. Power Appl.*, vol. 143, no. 6, pp. 429–436, Nov. 1996.
[59] W. M. Arshad, T. Backstrom, and C. Sadarangani, "Analytical design and analysis procedure for a transverse flux machine," in *Proc. IEMDC . IEEE Int. Electr. Mach. Drives Conf.*, Jun. 2001, pp. 115–121.
[60] W. M. Arshad, "Investigating a transverse flux machine with intermediate poles," in *Proc. Int. Conf. Power Electron. Mach. Drives*, 2002, pp. 325–328.
[61] D. Svechkarenko, J. Soulard, and C. Sadarangani, "A novel transverse flux generator in direct-driven wind turbines," in *Proc. Nordic Wksp. Power Ind. Electron.*, pp. 1–6, Jun. 2006.
[62] D. Svechkarenko, J. Soulard, and C. Sadarangani, "Analysis of a novel transverse flux generator in direct-driven wind turbines," in *Proc. Int. Conf. Electr., Mach.*, Sep. 2006, pp. 1–6.
[63] D. Svechkarenko, "On design and analysis of a novel transverse flux generator for direct-driven wind application," Ph.D. dissertation, Dept. Elect. Mach. Power Electron., KTH Roy. Inst. Tech., Stockholm, Sweden, 2010.
[64] G. Kastinger, "Design of a novel transverse flux machine," in *Proc. Int. Conf. Electr., Mach.*, Bruges, Belgium, 2002, pp. 1–6.
[65] J. F. Gieras, "Performance characteristics of a transverse flux generator," in *Proc. IEEE Int. Conf. Electric Mach. Drives*, May 2005, pp. 1293–1299.
[66] O. Dobzhanskyi, "Study on permanent magnet transverse flux machine," Ph.D. dissertation, Dept. Elect. Comput. Eng., Louisiana State Univ., Baton Rouge, LA, USA, 2012.
[67] M. A. Patel and S. C. Vora, "Analysis of a fall-back transverse-flux permanent-magnet generator," *IEEE Trans. Magn.*, vol. 53, no. 11, pp. 1–5, Nov. 2017.
[68] D. Svechkarenko, J. Soulard, and C. Sadarangani, "Parametric study of a transverse flux wind generator at no-load using three-dimensional finite element analysis," in *Proc. Int. Conf. Electr. Mach. Syst.*, Nov. 2009, pp. 1–6.
[69] G. Henneberger, "Development of a new transverse flux motor," in *Proc. IEE Colloq. New Topologies Permanent Magnet Mach.*, 1997, pp. 1–6.
[70] M. F. J. Kremers, "Analytical design of a transverse flux machine," Ph.D. dissertation, Dept. Elect. Eng., Eindhoven Univ. Tech., Eindhoven, The Netherlands, 2016.
[71] H. Weh, "Transverse flux (TF) machines in drive and generator application," in *Proc. IEEE Intt. Symp. Electr. Power Eng. Power Tech.*, Stockholm, Sweden, Jun. 1995, pp. 75–80.
[72] H. Weh and H. May, "Achievable force densities for permanent magnet excited machines in new configurations," in *Proc. Int. Conf. Electr., Mach. Drives*, Sep. 1986, pp. 1107–1111.
[73] E. Muljadi, C. P. Butterfield, and Y.-H. Wan, "Axial-flux modular permanent-magnet generator with a toroidal winding for wind-turbine applications," *IEEE Trans. Ind. Appl.*, vol. 35, no. 4, pp. 831–836, Jul. 1999.
[74] S. K. T. Lundmark, "Application of 3-D computation of magnetic fields to the design of claw pole motors," Ph.D. dissertation, Dept. Energy Environ., Chalmers Univ. Tech., Gothenburg, Sweden, 2005.
[75] C. P. Maddison, B. C. Mecrow, and A. G. Jack, "Claw pole geometries for high performance transverse flux machine," in *Proc. Int. Conf. Electr., Mach.*, Istanbulr, Turkey, vol. 1, Sep. 1998, pp. 340–345.
[76] F. Dreher and N. Parspour, "A novel high-speed permanent magnet claw pole transverse flux machine for use in automation," in *Proc. Int. Symp. Power Electron. Power Electron., Electr. Drives, Autom. Motion*, Jun. 2012, pp. 1240–1245.
[77] A. Ahmed, Z. Wan, and I. Husain, "Permanent magnet transverse flux machine with overlapping stator poles," in *Proc. IEEE Energy Convers. Congr. Expo. (ECCE)*, Sep. 2015, pp. 791–798.
[78] T. Husain, I. Hasan, Y. Sozer, I. Husain, and E. Muljadi, "A comprehensive review of permanent magnet transverse flux machines for direct drive applications," in *Proc. IEEE Energy Convers. Congr. Expo. (ECCE)*, Oct. 2017, pp. 1126–1255.
[79] M. Siatkowski and B. Orlik, "Flux linkage in transverse flux machines with flux concentration," in *Proc. 11th Int. Conf. Optim. Electr. Electron. Equip.*, May 2008, pp. 21–26.
[80] M. R. Dubois, "Transverse-flux permanent magnet (TFPM) machine with toothed rotor," in *Proc. Int. Conf. Power Electron. Mach. Drives*, Jun. 2002, pp. 309–314.
[81] F. T. V. Nica, E. Ritchie, and K. Leban, "A comparison between two optimized TFPM geometries for 5 MW direct-drive wind turbines," in *Proc. 8TH Int. Symp. Adv. TOPICS Electr. Eng. (ATEE)*, May 2013, pp. 1–6.
[82] D.-j. Bang, H. Polinder, G. Shrestha, and J. A. Ferreira, "Comparative design of radial and transverse flux PM generators for direct-drive wind turbines," in *Proc. 18th Int. Conf. Electr. Mach.*, Sep. 2008, pp. 1–6.
[83] D.-J. Bang, H. Polinder, G. Shrestha, and J. A. Ferreira, "Design of a lightweight transverse flux permanent magnet machine for direct-drive wind turbines," in *Proc. IEEE Ind. Appl. Soc. Annu. Meeting*, Oct. 2008, pp. 1–7.
[84] J. Jung, S. Ulbrich, and W. Hofmann, "Design process of a high torque density direct drive involving a transverse flux machine," in *Proc. Int. Conf. Electr. Mach. (ICEM)*, Sep. 2014, pp. 1096–1102.
[85] P. Zheng, Q. Zhao, J. Bai, B. Yu, Z. Song, and J. Shang, "Torque density improvement of transverse-flux dual rotor machine for power-split hybrid electric vehicle application," in *Proc. 17th Int. Conf. Electr. Mach. Syst. (ICEMS)*, Oct. 2014, pp. 1178–1182.
[86] S. Baserrah and B. Orlik, "Comparison study of permanent magnet transverse flux motors (PMTFMs) for in-wheel applications," in *Proc. Int. Conf. Power Electron. Drive Syst. (PEDS)*, Nov. 2009, pp. 96–101.
[87] N. J. Baker and S. Jordan, "Comparison of two transverse flux machines for an aerospace application," *IEEE Trans. Ind. Appl.*, vol. 54, no. 6, pp. 5783–5790, Nov. 2018.
[88] M. R. Dubois, H. Polinder, and J. A. Ferreira, "Prototype of a new transverse-flux permanent magnet (TFPM) machine with toothed rotor," in *Proc. Int. Conf. Electr., Mach.*, Aug. 2002, pp. 1–6.
[89] H. Azarinfar and M. Aghaebrahimi, "Design, analysis and fabrication of a novel transverse flux permanent magnet machine with disk rotor," *Appl. Sci.*, vol. 7, no. 8, p. 860, Aug. 2017.
[90] H. Weh, H. Hoffman, J. Landrath, H. Mosebach and J. Poschadel, "Directly driven permanent-magnet excited synchronous generator for variable speed operation," in *Proc. Eur. Community Wind Energy Conf.*, 1988, pp. 566–572.
[91] A. J. Mitcham, "Transverse flux motors for electric propulsion of ships," in *Proc. IEE Colloq. New Topologies for Permanent Magnet Mach.*, 1997, pp. 1–3.

[92] Y. Rang, C. Gu, and H. Li, "Analytical design and modeling of a transverse flux permanent magnet machine," in *Proc. Int. Conf. Power Syst. Technol.*, Oct. 2002, pp. 2164–2167.

[93] M. R. Dubios, "Optimized permanent magnet generator topologies for direct-drive wind turbines," Ph. D. dissertation, Dept. Elect. Eng., Delf Univ., Delft, The Netherlands, 2004.

[94] T. Husain, I. Hasan, Y. Sozer, I. Husain, and E. Muljadi, "Design considerations of a transverse flux machine for direct-drive wind turbine applications," in *Proc. IEEE Energy Convers. Congr. Expo. (ECCE)*, Sep. 2016, pp. 1–8.

[95] T. Husain, I. Hasan, Y. Sozer, I. Husain, and E. Muljadi, "Design of a modular E-Core flux concentrating transverse flux machine," *IEEE Trans. Ind. Appl.*, vol. 54, no. 3, pp. 2115–2128, May 2018.

[96] Z. Wan, A. Ahmed, I. Husain, and E. Muljadi, "A novel transverse flux machine for vehicle traction aplications," in *Proc. IEEE Power Energy Soc. Gen. Meeting*, Jul. 2015, pp. 1–5.

[97] A. Tovar-Barranco, D. J. Gomez, A. Lopez-de-Heredia, and I. Villar, "High torque density transverse flux permanent magnet machine design for wind power generation," in *Proc. 22th Int. Conf. Electr. Mach. (ICEM)*, Sep. 2016, pp. 782–788.

[98] A. Njeh, A. Masmoudi, and A. Elantably, "3D FEA based investigation of the cogging torque of a claw pole transverse flux permanent magnet machine," in *Proc. IEEE Int. Electr. Mach. Drives Conf. IEMDC*, Jun. 2003, pp. 319–324.

[99] Y. Guo, J. G. Zhu, P. A. Watterson, and W. Wu, "Development of a PM transverse flux motor with soft magnetic composite core," *IEEE Trans. Energy Convers.*, vol. 21, no. 2, pp. 426–434, Jun. 2006.

[100] D.-J. Bang, H. Polinder, G. Shrestha, and J. A. Ferreira, "Ring-shaped transverse flux PM generator for large direct-drive wind turbines," in *Proc. Int. Conf. Power Electron. Drive Syst. (PEDS)*, Nov. 2009, pp. 61–66.

[101] J. Xie, S. Zhao, and J. Li, "Research on key techniques of green mechanical press directly driven by transverse flux machine," in *Proc. IEEE Int. Conf. Mechatronics Autom.*, Aug. 2010, pp. 1381–1386.

[102] C. Pompermaier, L. Sjoberg, and G. Nord, "Design and optimization of a permanent magnet transverse flux machine," in *Proc. 20th Int. Conf. Electr. Mach.*, Sep. 2012, pp. 606–611.

[103] J. Yan, H. Lin, Y. Huang, H. Liu, and Z. Q. Zhu, "Magnetic field analysis of a novel flux switching transverse flux permanent magnet wind generator with 3-D FEM," in *Proc. Int. Conf. Power Electron. Drive Syst. (PEDS)*, Nov. 2009, pp. 1–4.

[104] C. Liu, G. Lei, B. Ma, Y. Wang, Y. Guo, and J. Zhu, "Development of a new low-cost 3-D flux transverse flux FSPMM with soft magnetic composite cores and ferrite magnets," *IEEE Trans. Magn.*, vol. 53, no. 11, pp. 1–5, Nov. 2017.

[105] Z. Wan and I. Husain, "Design, analysis and prototyping of a flux switching transverse flux machine with ferrite magnets," in *Proc. IEEE Energy Convers. Congr. Expo. (ECCE)*, Oct. 2017, pp. 1227–1233.

[106] Z. Wan and I. Husain, "Design of a flux switching transverse flux machine based on generalized inductance analysis," in *Proc. IEEE Int. Electr. Mach. Drives Conf. (IEMDC)*, May 2017, pp. 1–6.

[107] Y. Ueda, H. Takahashi, A. Ogawa, T. Akiba, and M. Yoshida, "Cogging-torque reduction of transverse-flux motor by skewing stator poles," *IEEE Trans. Magn.*, vol. 52, no. 7, pp. 1–4, Jul. 2016.

[108] B. Ren, G.-J. Li, Z.-Q. Zhu, M. Foster, and D. Stone, "Performance comparison between consequent-pole and inset modular permanent magnet machines," *J. Eng.*, vol. 2019, no. 17, pp. 3951–3955, Jun. 2019.

[109] Y. Ueda, H. Takahashi, T. Akiba, and M. Yoshida, "Fundamental design of a consequent-pole transverse-flux motor for direct-drive systems," *IEEE Trans. Magn.*, vol. 49, no. 7, pp. 4096–4099, Jul. 2013.

[110] X. Zhao and S. Niu, "Design of a novel consequent-pole transverse-flux machine with improved permanent magnet utilization," *IEEE Trans. Magn.*, vol. 53, no. 11, pp. 1–5, Nov. 2017.

[111] I. Hassan, "Modeling and analysis of high torque density transverse flux machines for direct-drive applications," Ph.D. dissertation, Dept. Elect. Comput. Eng., Akron Univ., Akron, OH, USA, 2017.

[112] H. Weh and J. Jiang, "Calculation and design consideration for synchronous machines with transverse flux configuration," *Archiv Für Elektrotechnik*, vol. 71, pp. 187–198, 1988.

[113] A. Zavvos, D. Bang, A. S. McDonald, H. Polinder, and M. Mueller, "Structural analysis and optimisation of transverse flux permanent magnet machines for 5 and 10 MW direct drive wind turbines," *Wind Energy*, vol. 15, no. 1, pp. 19–43, Jan. 2012.

[114] M. R. Dubois, H. Polinder, and J. A. Ferreira, "Influence of air gap thickness in transverse flux permanent magnet (TFPM) generators for wind turbine application," in *Proc. IEEE Young Researchers Symp. Electr. Power Eng.*, 2002, pp. 1–7.

[115] R. Kumar, Z. Q. Zhu, A. Duke, A. Thomas, and R. Clark, "Influence of air gap in transverse flux permanent magnet machine for wind power applications," presented at the Int. Conf. Electric. Mach., Gothenburg, Sweden, Aug. 2020.

[116] M. R. Harris, G. H. Pajooman, and S. M. Abu Sharkh, "The problem of power factor in VRPM (transverse-flux) machines," in *Proc. 8th Int. Conf. Electr. Mach. Drives*, 1997, pp. 90–386.

[117] J. Renedo Anglada and S. M. Sharkh, "An insight into torque production and power factor in transverse-flux machines," *IEEE Trans. Ind. Appl.*, vol. 53, no. 3, pp. 1971–1977, Jun. 2017.

[118] K. Y. Lu, E. Ritchie, P. O. Rasmussen, and P. Sandholdt, "Modeling and power factor analysis of a single phase surface mounted permanent magnet transverse flux machine," in *Proc. 5th Int. Conf. Power Electron. Drive Syst. PEDS*, Nov. 2003, pp. 1609–1613.

[119] A. Zaidi, L. Senn, I. Ortega, P. Radecki, I. Szczesny, M. Erkec, E. Ritchie, and K. Leban, "5MW direct drive wind turbine generator design," in *Proc. 20th Int. Conf. Electr. Mach.*, Sep. 2012, pp. 1140–1145.

[120] A. Ahmed and I. Husain, "Power factor improvement of a transverse flux machine with high torque density," in *Proc. IEEE Int. Electric Mach. Drives Conf. (IEMDC)*, May 2017, pp. 1–6.

[121] P. Anpalahan, J. Soulard, and H.-P. Nee, "Design steps towards a high power factor transverse flux machine," in *Proc. Eur. Conf. Power Electron. Appl.*, Aug. 2001, pp. 1–6.

[122] D. S. Drennan, "Design of a passive rotor transverse flux rotating machine," M.S. thesis, Dept. Elect. Electron. Eng., Stellenbosch Univ., Stellenbosch, South Africa, Apr. 2005.

[123] T. Husain, I. Hasan, Y. Sozer, I. Husain, and E. Muljadi, "Cogging torque minimization in transverse flux machines," in *Proc. IEEE Energy Convers. Congr. Expo. (ECCE)*, Sep. 2016, pp. 1–8.

[124] N. Bianchi and S. Bolognani, "Design techniques for reducing the cogging torque in surface-mounted PM motors," *IEEE Trans. Ind. Appl.*, vol. 38, no. 5, pp. 1259–1265, Sep. 2002.

[125] F. Dreher and N. Parspour, "Reducing the cogging torque of PM transverse flux machines by discrete skewing of a segmented stator," in *Proc. 20th Int. Conf. Electr. Mach.*, Sep. 2012, pp. 454–457.

[126] A. B. Letelier, D. A. Gonzalez, J. A. Tapia, R. Wallace, and M. A. Valenzuela, "Cogging torque reduction in an axial flux PM machine via stator slot displacement and skewing," *IEEE Trans. Ind. Appl.*, vol. 43, no. 3, pp. 685–693, May 2007.

[127] G. Kastinger, "Reducing torque ripple of transverse flux machines by structural designs," in *Proc. Int. Conf. Power Electron. Mach. Drives*, 2002, pp. 320–324.

[128] J.-Y. Lee, J.-H. Chang, D.-H. Kang, S.-I. Kim, and J.-P. Hong, "Tooth shape optimization for cogging torque reduction of transverse flux rotary motor using design of experiment and response surface methodology," *IEEE Trans. Magn.*, vol. 43, no. 4, pp. 1817–1820, Apr. 2007.

[129] Z. Jia, H. Lin, S. Fang, and Y. Huang, "Cogging torque optimization of novel transverse flux permanent magnet generator with double C-Hoop stator," *IEEE Trans. Magn.*, vol. 51, no. 11, pp. 1–4, Nov. 2015.

[130] H. Ahn, G. Jang, J. Chang, S. Chung, and D. Kang, "Reduction of the torque ripple and magnetic force of a rotatory two-phase transverse flux machine using herringbone teeth," *IEEE Trans. Magn.*, vol. 44, no. 11, pp. 4066–4069, Nov. 2008.

[131] P. M. Golatgaonkar, B. N. Chaudhari, and R. T. Ugale, "Torque ripple reduction in a homo-polar poly-phase transverse flux machine," in *Proc. 9th Int. Conf. Power Electron. Mach. Drives.*, Apr. 2018, pp. 1–6.

[132] Y. Guo, J. Zhu, H. Lu, S. Wang, and J. Jin, "Performance analysis of an SMC transverse flux motor with modified double-sided stator and PM flux concentrating rotor," in *Proc. Int. Conf. Electr., Mach. Syst.*, Seoul South Korea, Oct. 2007, pp. 1553–1556.

[133] J. Chang, J. Lee, J. Kim, S. Chung, D. Kang, and H. Weh, "Development of rotating type transverse flux machine," in *Proc. IEEE Int. Electric Mach. Drives Conf.*, May 2007, pp. 1090–1095.

[134] S. Jordan and N. J. Baker, "Design and build of a mass critical, air-cooled transverse flux machine for aerospace," in *Proc. 20th Int. Conf. Electr. Mach. (ICEM)*, Sep. 2016, pp. 1453–1458.

[135] G. Q. Bao, J. H. Shi, and J. Z. Jiang, "Efficiency optimization of transverse flux permanent magnet machine using genetic algorithm," in *Proc. Int. Conf. Electr. Mach. Syst.*, Sep. 2005, pp. 380–384.

[136] S. Muller, M. Siegle, M. Keller, and N. Parspour, "Loss calculation for electrical machines based on finite element analysis considering 3D magnetic flux," in *Proc. 13th Int. Conf. Electr. Mach. (ICEM)*, Sep. 2018, pp. 1246–1252.
[137] S. Baserrah and B. Orlik, "Eddy current investigation study for a non-conventional flux concentrated permanent magnet transverse flux machine using finite element method via 3D transient approach," in *Proc. IEEE Int. Electr. Mach. Drives Conf. (IEMDC)*, May 2011, pp. 47–52.
[138] J.-Y. Lee, D.-H. Kang, J.-H. Jang, and J.-P. Hong, "Rapid eddy current loss calculation for transverse flux linear motor," in *Proc. Conf. Rec. IEEE Ind. Appl. Conf. 41st IAS Annu. Meeting*, Oct. 2006, pp. 400–406.
[139] L. Strete, L. Tutelea, I. Boldea, C. Martis, and I.-A. Viorel, "Optimal design of a rotating transverse flux motor (TFM) with permanent magnets in rotor," in *Proc. 21th Int. Conf. Electr. Mach. - ICEM*, Sep. 2010, pp. 1–6.
[140] M. Bork and G. Henneberger, "New transverse flux concept for an electric vehicle drive system," in *Proc. Int. Conf. Electric. Machi.*, Vigo, Spain, vol. 2, Sep. 1996, pp. 308–313.
[141] K. Lu, P. O. Rasmussen, and E. Ritchie, "Design considerations of permanent magnet transverse flux machines," *IEEE Trans. Magn.*, vol. 47, no. 10, pp. 2804–2807, Oct. 2011.
[142] S. Huang, J. Luo, and T. A. Lipo, "Analysis and evaluation of the transverse flux circumferential current machine," in *Proc. IAS Conf. Rec. IEEE Ind. Appl. Conf. 32nd IAS Annu. Meeting*, Oct. 1997, pp. 378–384.
[143] A. M. A. Elantably, "An approach to sizing high power density TFPM intended for hybrid bus electric propulsion," *Electr. Mach. Power Syst.*, vol. 28, no. 4, pp. 341–354, Apr. 2000.
[144] Z. Yu and C. Jianyun, "Power factor analysis of transverse flux permanent machines," in *Proc. Int. Conf. Electr. Mach. Syst.*, Sep. 2005, pp. 450–459.
[145] Y. Tang, J. J. H. Paulides, and E. A. Lomonova, "Analytical modeling of flux-switching in-wheel motor using variable magnetic equivalent circuits," *ISRN Automot. Eng.*, vol. 2014, pp. 1–10, Jan. 2014.
[146] A. Babazadeh, N. Parspour, and A. Hanifi, "Transverse flux machine for direct-drive robots: Modelling and analysis," in *Proc. IEEE Conf. Robot. Autom. Mech.*, vol. 1, Dec. 2004, pp. 376–380.
[147] M. F. J. Kremers, J. J. H. Paulides, J. L. G. Janssen, and E. A. Lomonova, "Analytical flux linkage and EMF calculation of a transverse flux machine," in *Proc. Int. Conf. Electr. Mach. (ICEM)*, Sep. 2014, pp. 2668–2673.
[148] M. Zafarani, M. Moallem, and A. Tabesh, "Analytical model for a transverse flux permanent magnet machine using improved magnetic equivalent circuit approach," in *Proc. 21st Int. Conf. Syst. Eng.*, Aug. 2011, pp. 96–99.
[149] P. Seibold and N. Parspour, "Analytical computation method of transverse flux permanent magnet excited machines via nodal analysis," in *Proc. Int. Conf. Electr. Mach. (ICEM)*, Sep. 2014, pp. 410–415.
[150] I. Hasan, T. Husain, M. W. Uddin, Y. Sozer, I. Husain, and E. Muljadi, "Analytical modeling of a novel transverse flux machine for direct drive wind turbine applications," in *Proc. IEEE Energy Convers. Congr. Expo. (ECCE)*, Sep. 2015, pp. 2161–2168.
[151] J. R. Anglada and S. M. Sharkh, "Analytical calculation of air-gap magnetic field distribution in transverse-flux machines," in *Proc. IEEE 25th Int. Symp. Ind. Electron. (ISIE)*, Jun. 2016, pp. 141–146.
[152] B. E. Hasubek and E. P. Nowicki, "Two dimensional finite element analysis of passive rotor transverse flux motors with slanted rotor design," in *Proc. Eng. Solutions Next Millennium. IEEE Can. Conf. Electr. Comput. Eng.*, May 1999, pp. 1199–1204.
[153] C. P. Maddison, "Transverse flux machines for high torque applications," Ph.D. dissertation, Dept. Elect. Electron. Eng., Newcastle Univ., Newcastle upon Tyne, U.K., 1999.
[154] O. Dobzhanskyi, E. E. Mendrela, and A. M. Trzynadlowski, "Analysis of leakage flux losses in the transverse flux permanent magnet generator," in *Proc. IEEE Green Technol. Conf. (IEEE-Green)*, Apr. 2011, pp. 1–6.
[155] B. Zhang, A. Wang, and M. Doppelbauer, "Multi-objective optimization of a transverse flux machine with claw-pole and flux-concentrating structure," *IEEE Trans. Magn.*, vol. 52, no. 8, pp. 1–10, Aug. 2016.
[156] D.-J. Bang, "Design of transverse flux permanent magnet machines for large direct-drive wind turbines," Ph.D. disseration, Dept. Elect. Sustain. Energy, Delft Univ., Delft The Netherlands, 2010.
[157] M. Nell, J. Lenz, and K. Hameyer, "Scaling laws for the FE solutions of induction machines," *J. Electr., Eng.*, vol. 68, no. 03, pp. 677–695, 2019.
[158] H. Li, Z. Chen, and H. Polinder, "Optimization of multibrid permanent-magnet wind generator systems," *IEEE Trans. Energy Convers.*, vol. 24, no. 1, pp. 82–92, Mar. 2009.
[159] A. Ejlali, J. Soleimani, and A. Vahedi, "Review in transverse flux permanent magnet generator design," *Iran. J. Electr., Electron.*, vol. 12, no. 4, pp. 257–269, 2016.
[160] S. Hosseini, J. S. Moghani, N. F. Ershad, and B. B. Jensen, "Design, prototyping, and analysis of a novel modular permanent-magnet transverse flux disk generator," *IEEE Trans. Magn.*, vol. 47, no. 4, pp. 772–780, Apr. 2011.
[161] M. B. C. Salles, J. R. Cardoso, and K. Hameyer, "Dynamic modeling of transverse flux permanent magnet generator for wind turbines," *J. Microw., Optoelectron. Electromagn. Appl.*, vol. 10, no. 1, pp. 95–105, Jun. 2011.
[162] Devashish, A. Thakur, S. Panigrahi, and R. R. Behera, "A review on wind energy conversion system and enabling technology," in *Proc. Int. Conf. Electr. Power Energy Syst. (ICEPES)*, Dec. 2016, pp. 527–532.
[163] B. Jain, S. Jain, and R. K. Nema, "Control strategies of grid interfaced wind energy conversion system: An overview," *Renew. Sustain. Energy Rev.*, vol. 47, pp. 983–996, Jul. 2015.
[164] M. S. Merzoug and F. Naceri, "Comparison of field oriented control and direct torque control for PMSM," *World Acad. Sci. Eng. Tech.*, vol. 21, pp. 209–304, Nov. 2008.
[165] R. Tiwari and N. R. Babu, "Recent developments of control strategies for wind energy conversion system," *Renew. Sustain. Energy Rev.*, vol. 66, pp. 268–285, Dec. 2016.
[166] N. Freire, J. Estima, and A. Cardoso, "A comparative analysis of PMSG drives based on vector control and direct control techniques for wind turbine applications," *Przeglad Elektrotechniczny*, vol. 88, no. 1A, pp. 184–187, 2012.
[167] M. Allagui, O. B. K. Hasnaoui, and J. Belhadj, "A 2MW direct drive wind turbine; vector control and direct torque control techniques comparison," *J. Energy Southern Afr.*, vol. 25, no. 2, pp. 117–126, Jun. 2014.
[168] G. Lei, Y. G. Guo, J. G. Zhu, T. S. Wang, X. M. Chen, and K. R. Shao, "System level six sigma robust optimization of a drive system with PM transverse flux machine," *IEEE Trans. Magn.*, vol. 48, no. 2, pp. 923–926, Feb. 2012.
[169] M. Keller and N. Parspour, "Experimental identification and validation of model parameters of a permanent magnetic excited transverse flux machine for robotic applications," in *Proc. 11th IEEE Int. Conf. Compat., Power Electron. Power Eng. (CPE-POWERENG)*, Apr. 2017, pp. 352–357.
[170] M. Siatkowski, J. Schuttler, and B. Orlik, "FEM-data based model for fast simulation of a transverse flux machine," in *Proc. 21th Int. Conf. Electr. Mach. ICEM*, Sep. 2010, pp. 1–6.
[171] N. Taib, B. Metidji, and T. Rekioua, "A fixed switching frequency direct torque control strategy for induction motor drives using indirect matrix converters," *Arabian J. Sci. Eng.*, vol. 39, pp. 2001–2011, Mar. 2014.
[172] X. Tu, Y. Dai, and C. Gu, "Direct torque and adaptive flux control of novel transverse-flux permanent magnet motor with brushless DC drive," in *Proc. 15th Int. Conf. Electr., Mach. Syst.*, Oct. 2012, pp. 1–4.
[173] C. Zhang, M. Jiang, W. Gao, and X. Guo, "An improved scheme of fuzzy direct torque control of transverse flux permanent-magnet machine," *J. Comput. Inf. Syst.*, vol. 8, no. 1, pp. 125–133, 2012.
[174] D. K. K. Padinharu, G.-J. Li, Z.-Q. Zhu, R. Clark, A. S. Thomas, and Z. Azar, "System-level investigation of multi-MW direct-drive wind power PM Vernier generators," *IEEE Access*, vol. 8, pp. 191433–191446, 2020.
[175] N. A. Bhuiyan and A. McDonald, "Optimization of offshore direct drive wind turbine generators with consideration of permanent magnet grade and temperature," *IEEE Trans. Energy Convers.*, vol. 34, no. 2, pp. 1105–1114, Jun. 2019.
[176] P. Chimurkar and P. Kothavade, "A review of different power converter topologies for PMSGs wind turbine," in *Proc. Int. Conf. Commun. Electron. Syst. (ICCES)*, Oct. 2016, pp. 1–6.
[177] M. R. Islam, Y. Guo, and J. Zhu, "Power converters for wind turbines: Current and future development," in *Materials and Processes for Energy: Communicating Current Research and Technological Developments* (Energy Book Series). Badajoz, Spain: Formatex Research Centre, 2013, pp. 559–571. [Online]. Available: https://www.researchgate.net/publication/262974138_Power_converters_for_wind_turbines_Current_and_future_development
[178] V. Yaramasu, B. Wu, P. C. Sen, S. Kouro, and M. Narimani, "High-power wind energy conversion systems: State-of-the-art and emerging technologies," *Proc. IEEE*, vol. 103, no. 5, pp. 740–788, May 2015.
[179] M. Jamil, R. Gupta, and M. Singh, "A review of power converter topology used with PMSG based wind power generation," in *Proc. IEEE 5th Power India Conf.*, Dec. 2012, pp. 1–6.

RAJESH KUMAR (Member, IEEE) was born in Umerkot, Pakistan. He received the B.E. degree in industrial electronics from the Institute of Industrial Electronics Engineering, Karachi, Pakistan, in 2013, and the M.Sc. degree in electrical engineering from the University of Tun Hussein Onn, Malaysia, in 2017. He is currently pursuing the Ph.D. degree in electrical engineering with The University of Sheffield, U.K. His research interests include design, modeling, and optimization of permanent magnet machines.

ZI-QIANG ZHU (Fellow, IEEE) received the B.Eng. and M.Sc. degrees in electrical and electronic engineering from Zhejiang University, Hangzhou, China, in 1982 and 1984, respectively, and the Ph.D. degree in electronic and electrical engineering from The University of Sheffield, Sheffield, U.K., in 1991. Since 1988, he has been with The University of Sheffield, where he currently holds the Royal Academy of Engineering/Siemens Research Chair. He is also the Head of the Electrical Machines and Drives Research Group, the Academic Director of the Sheffield Siemens Gamesa Renewable Energy Research Centre, the Director of the CRRC Electric Drives Technology Research Centre, and the Director of the Midea Electric Machines and Control Research Centre. His research interests include design and control of permanent-magnet brushless machines and drives for applications ranging from automotive through domestic appliances to renewable energy. He is a Fellow of the Royal Academy of Engineering.

ALEXANDER DUKE received the M.Eng. and Ph.D. degrees in electrical engineering from The University of Sheffield, U.K., in 2011 and 2015, respectively. Since 2016, he has been with the Siemens Gamesa Renewable Energy Research Centre, where he is currently an Advanced Engineer specializing in the electromagnetic design of permanent magnet wind power generators.

ARWYN THOMAS received the M.Eng. and Ph.D. degrees in electronic and electrical engineering from The University of Sheffield, Sheffield, U.K., in 2005 and 2009, respectively. He is currently the Head of Generator Technology Development with the Siemens Gamesa Renewable Energy Research Centre, Sheffield. His research interests include modeling, design, and analysis of permanent magnet brushless machines.

RICHARD CLARK received the B.Eng. degree in electrical engineering from The University of Sheffield and the Ph.D. degree, in 1999, for research on permanent magnet actuators. He was a Postdoctoral Research Associate. He was a Lecturer in electrical engineering with The University of Sheffield, in 2005. He joined Magnomatics, The University of Sheffield, spin-out company developing novel electrical motors and generators and magnetic transmissions, in 2007, where he held posts of a Research and Development Manager, a Research Director, and a Principal Engineer. He joined the Siemens Gamesa Renewable Energy Research Centre, Sheffield, U.K., as an Electromagnetic Specialist, in October 2017. He was awarded a five year Royal Academy of Engineering Research Fellowship.

ZIAD AZAR received the B.Eng. degree in electrical engineering from the University of Damascus, Damascus, Syria, in 2003, and the M.Sc. degree in electronic and electrical engineering and the Ph.D. degree in electrical engineering from The University of Sheffield, Sheffield, U.K., in 2008 and 2012, respectively. His Ph.D. studies include the modeling, design, and analysis of permanent-magnet and magnetless brushless machines for automotive applications. He joined the Siemens Gamesa Renewable Energy Research Centre, in 2012, where he is currently the Generator Team Manager with the Technology Development Department, and the focus has been on maturing and developing of new technologies for direct-drive wind power generators.

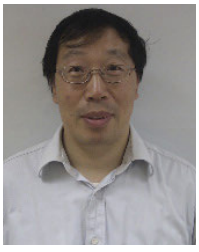

ZHAN-YUAN WU received the B.Eng. and M.Sc. degrees in electrical engineering from Northeastern University, Shenyang, China, in 1985 and 1988, respectively, and the Ph.D. degree from The University of Sheffield, Sheffield, U.K., in 1999. He is currently working with the Siemens Gamesa Renewable Energy Research Centre. His main research interests include control of permanent-magnet brushless machines and drives.